

SELF ASSEMBLING POROUS LOW-K
DIELECTRIC THIN FILMS

THESIS

Presented to the Graduate Council
of Texas State University-San Marcos
in Partial Fulfillment
of the Requirements

for the Degree
Masters of Science

by

William Thomas Gibson, A.S., B.S.

San Marcos, Texas

May 2006

COPYRIGHT

by

William Thomas Gibson, A.S., B.S.

2006

DEDICATION

For: Amy, Mom, Dad, Suzanne, and Tiger

ACKNOWLEDGEMENTS

I would like to thank the following: Texas State University-San Marcos, Physics Department for providing me a home, my thesis committee for all their support and assistance, and my fellow students in Dr. Galloway's research group for all their help. In addition, I would like to thank the Texas State University-San Marcos, Department of Chemistry and Biochemistry for the use of their equipment and facilities as well as the Albert B. Alkek library especially the office of interlibrary loans. I owe an additional thanks to Ms. Jacqueline P. Smits, Department of Chemistry and Biochemistry, for all of her assistance with the toluene still; Ms. Patricia J. Parks, Department of Physics, for keeping me in the information loop. Additional thanks to Dr. Galloway, the threats of physical harm did help. Finally, thank you to my family for all their support and patience.

This manuscript was submitted on April 6, 2006

TABLE OF CONTENTS

	Page
ACKNOWLEDGEMENTS	v
LIST OF EQUATIONS	viii
LIST OF TABLES	ix
LIST OF FIGURES	x
ABSTRACT	xii
CHAPTER	
I MOTIVATION	1
Crosstalk	1
Use of Polymers	4
II INTRODUCTION/THEORY	6
Low- κ Materials	6
Atomic Force Microscopy	8
Fourier Transform Infrared Spectroscopy	13
Polymers	15
Random Copolymer	17
Diblock Copolymer	18
Cleaning	20
Standard Cleans	21
Ultrasonic Cleaning	23
III PROCEDURES	25
Consumables List	25
Substrate Preparation	27
Glove Box	29
Spin Casting	30
Polymer Preparations	31
Random Copolymer	32
Diblock Copolymer	33
Atomic Force Microscopes	34
Park Scientific (Contact Mode)	34
Veeco (Contact and Tapping Modes)	34
Ultrasonic Cleaner	36

Fourier Transform Infrared Spectroscopes.....	37
Bomem	38
Nicolet 6700	38
Ultraviolet Radiation	38
Cleaning Study	39
IV RESULTS	41
Fourier Transform Infrared (FTIR) Qualification	41
Cleaning Study	47
Random Copolymer Brushes.....	53
Diblock Copolymer Application	55
V CONCLUSIONS.....	57
APPENDICES	
(A) Toluene Distillation	59
(B) Standard Cleans Procedures.....	62
(C) Spinner Operation	65
(D) Glove Box Operation	68
(E) Ultrasonic Cleaner Operation	70
(F) Vacuum Oven Operation	72
(G) Polymer Preparation.....	74
REFERENCES	76
IMAGE REFERENCES	80

LIST OF EQUATIONS

	Page
Equation 1 Telegrapher's Equation Inductance.....	2
Equation 2 Telegrapher's Equation Capacitance.....	2
Equation 3 Capacitance Parallel Wires	3
Equation 4 Lorentz-Lorenz Equation	4
Equation 5 Dielectric Constant in Terms of the Lorentz-Lorenz Equation.....	4
Equation 6 Bruggeman Effective Medium Approximation	7
Equation 7 Number Average Molecular Weight.....	15
Equation 8 Weight Average molecular Weight.....	15
Equation 9 Polydispersity Index.....	15

LIST OF TABLES

	Page
Table 1 Classical Bond polarizabilities	4
Table 2 Dielectric Values for Various Materials.....	6
Table 3 T_g by % PMMA in a Copolymer with PS	17
Table 4 Compressed Gas Specifications	25
Table 5 Chemical Specifications	25
Table 6 Diblock Copolymer Specifications	26
Table 7 Random Copolymer Specifications.....	26
Table 8 Chemical for Standard Cleans.....	62
Table 9 Compressed Gas Specifications	68

LIST OF FIGURES

	Page
FIGURE 1 Simplified Model of Parasitic Effects	3
FIGURE 2 AFM Scanner Map	8
FIGURE 3 Piezo Scanner Tube	9
FIGURE 4 AFM Cantilever Deflection Detection Mechanism	10
FIGURE 5 AFM Tip Effects on Image	11
FIGURE 6 AFM Scanning Modes	12
FIGURE 7 Possible Atomic Vibrations for FTIR	14
FIGURE 8 Methyl Methacrylate and Styrene Monomers (MDL-model)	15
FIGURE 9 Methyl Methacrylate and Styrene Polymers (MDL-model)	16
FIGURE 10 OH Terminated Random Copolymer (RCP) (MDL-model)	18
FIGURE 11 Diblock Copolymer (DBC) (MDL-model)	19
FIGURE 12 Mechanisms of Cleaning	20
FIGURE 13 Isopropyl Alcohol (IPA) Drying Tool	22
FIGURE 14 Marangoni Drying Tool	23
FIGURE 15 Cavitation Jets Associated with Ultrasonic Cleaning	24
FIGURE 16 Substrate Separation and Identification	27
FIGURE 17 Glove Box and Control Electronics	29
FIGURE 18 Spinner and Control Panel	30
FIGURE 19 Spinner Vacuum Chuck / Vacuum Chuck with Sample	30
FIGURE 20 Vacuum Oven and Pump	33
FIGURE 21 Park Scientific AFM and Scanner Head	34
FIGURE 22 Veeco AFM and Scanner Head	35
FIGURE 23 Ultrasonic Cleaning System	36
FIGURE 24 FTIR Spectra: Testing RCP Detection	42

ABSTRACT

SELF-ASSEMBLING POROUS LOW-K DIELECTRIC THIN FILMS

by

William Thomas Gibson,^a A.S., B.S.

Texas State University-San Marcos

May 2006

SUPERVISING PROFESSOR: HEATHER C. GALLOWAY

Due to the increases in processing speeds and miniaturization demands placed on integrated circuits the traditional on chip insulator of silicon oxide $\kappa \approx 3.9$ allows crosstalk between interconnects. This crosstalk is detrimental to device performance, reducing the effective performance speed. One approach to reducing the crosstalk is to reduce the parasitic capacitance between the interconnects. To this end, we attempt to produce self-assembling thin films of polystyrene (PS) and polymethyl methacrylate (PMMA), to be used as a porous low- κ dielectric, on amorphous silicon carbide on silicon (SiC) and on silicon oxide on silicon (SiO₂). In the process, we optimized the deposition procedures for a 55% PS random copolymer (RCP). Also, we compared ultrasonic cleaning in an acetone bath with standard clean 1 and 2 (SC-1, SC-2) for SiC, SiO₂, and amorphous silicon carbon nitride on silicon (SiCN). This was a preliminary

step in surface preparation prior to deposition of the RCP. We identified an effective method of verifying the successful deposition of an RCP using fourier transform infrared spectroscopy (FTIR). We also successfully cast a diblock copolymer (DBC) of P(S-b-MMA) with a PS content of 50.8% that produced lamellar structures. Analysis of the cleaning comparison, RCP and DBC deposition were accomplished using FTIR and atomic force microscopy (AFM) using both contact and non-contact imaging.

CHAPTER 1

MOTIVATION

The 2001 and subsequent International Technology Roadmap for Semiconductors (ITRS) identifies the “introduction of new materials to meet conductivity requirements and reduce the dielectric permittivity” as one of the top three challenges for interconnects. The introduction of a low dielectric permittivity or low- κ material is one method of reducing interconnect delay due to crosstalk.

Crosstalk

Crosstalk is a term used to describe the parasitic effects that occur in the parallel conductors of an integrated circuit. The definition of crosstalk comes from the telecommunications industry where capacitive coupling and mutual inductance can cause signal degradation.

These effects can be described using the telegrapher’s equations or for a general description, we can use a first order approximation of the capacitance for two parallel wires. All conductors have resistance at room temperature. All parallel conductors have a parasitic impedance and capacitance as shown in figure 1. The inherent resistance in the metal of the interconnect is a function of material resistivity, and the conductor’s size and length. These factors are controlled by choice of materials and the resolution of the lithography techniques. The capacitance is a function of the size of the conductors, their separation, and the dielectric separating them. We wish to fabricate a porous low- κ

dielectric to meet this requirement. A low- κ dielectric is one with a dielectric permittivity of less than 3.5. A porous structure introduces air pockets into the dielectric. These air pockets reduce the capacitance between the lines by introducing regions filled with air, which has a dielectric permittivity of approximately 1.

Traditionally silicon oxide (SiO_2) has been the material of choice for interconnect separation. With a static dielectric value of 3.9 to 4.5, SiO_2 is neither a low- κ dielectric nor is it a high- κ material, which is important for gate dielectrics. However, the ease of growth and robust nature of SiO_2 made it a natural choice for use in integrated circuits for both gate dielectrics and interconnect separation. The end of this multi purpose material is now becoming apparent. As interconnect distances are reduced to maximize the use of available area on each die, a dielectric permittivity of 3.9 is no longer acceptable. Increased processing speeds and the drive for miniaturization demand dielectric materials more efficient than SiO_2 for on chip insulators.

A large body of work exists for modeling interconnect delay or crosstalk.¹⁻⁸ Most models start from, or soon incorporate transmission line theory and the associated telegrapher's equations. Where v is voltage, L is inductance, i is current, R is resistance, C is capacitance, and G is conductance.

$$\frac{\partial}{\partial x} v(x,t) = -L \frac{\partial}{\partial t} i(x,t) - Ri(x,t) \quad \text{Equation 1}$$

$$\frac{\partial}{\partial x} i(x,t) = -C \frac{\partial}{\partial t} v(x,t) - Gv(x,t) \quad \text{Equation 2}$$

The math, of course, becomes very complex, and even for conditions where analytical solutions are possible, it is often easier to obtain experimental values. However the goal is not to model interconnect delay, as much as defeat it. Therefore, it will be acceptable

to have proof of the existing conditions that lead to interconnect delay. To do this we need only look as far as a simple model of two infinitely long parallel wires (figure 1). Obviously, this becomes an RLC circuit and is subject to all of the associated effects such as charging time delays, signal attenuation, and phase shifts. While there are many ways to address each effect, we will restrict our discussion to ways of coping with the parasitic capacitance. In equation 3 below, you can see the effect of the dielectric value on the capacitance. Here d is the separation of the wires and a is the outer diameter of the wires. Once a and d have been minimized the only remaining variable is the dielectric and reducing its value is the only method left to reduce the capacitance between interconnects.

$$C = \frac{\pi \epsilon_o \kappa}{\ln \left[\frac{d}{2a} + \sqrt{\left(\frac{d}{2a} \right)^2 - 1} \right]} \left(\frac{F}{m} \right)$$

Equation 3

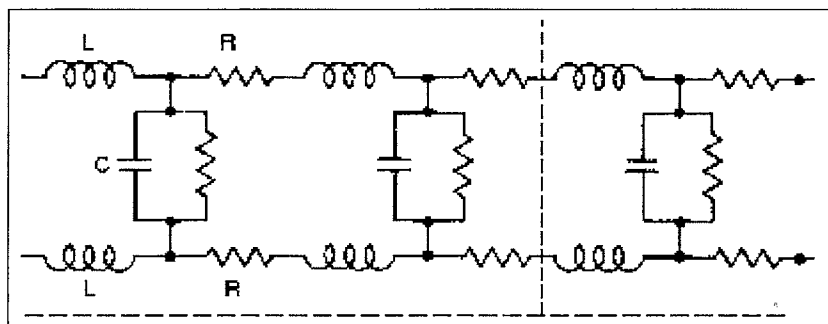


Figure 1 Simplified model of two infinitely long parallel conductors with parasitic effects demonstrated using their common electrical symbols. L is mutual inductance effects, C represents capacitance, and R is resistance.

Use of Polymers

Why would a polymer make a good low- κ material? Starting with the Lorentz-Lorenz equation (equation 4) and solving for κ (equation 5) we see the relative dielectric values to be a function of the number of elemental dipole moments N , and the polarizability of the elemental dipole moments α , where κ is the relative dielectric constant and ϵ_0 the permittivity of a vacuum. So that if we choose materials with

$$\alpha = \frac{3\epsilon_0(\kappa - 1)}{N(\kappa + 2)} \quad \text{Equation 4}$$

$$\kappa = \frac{1 + 2\left(\frac{N\alpha}{3\epsilon_0}\right)}{1 - \left(\frac{N\alpha}{3\epsilon_0}\right)} \quad \text{Equation 5}$$

small bond polarizabilities and a minimum number of double and triple bonds we have found a material with a low relative dielectric value. Table 1 lists some bond polarizabilities for different chemical bonds. From the information in table 1 it is apparent that fluorination or substituting fluorine for some of the hydrogen atoms would contribute to a reduced effective dielectric value for the material. This is because the replacement of hydrogen atoms not only reduces the bond polarizabilities but also prevents formation of additional double or triple bonds.

Classical Bond Polarizabilities ^b (Å ³)							
Bond Type	C-C	C-F	C-O	C-H	O-H	C=C	C≡C
Polarizability (Å ³)	0.531	0.555	0.584	0.652	0.706	1.643	2.036

Table 1 Classical bond polarizability (α) by bond type

In addition, the use of polymers for our low- κ dielectric is justified by their low processing temperatures. Therefore, they will have an insignificant effect on the thermal

budget of the IC. Second, the self-ordering behavior of thin film copolymers are an effective method for constructing nano-scale features. Third, our choice of polystyrene block polymethyl methacrylate [P(S-b-MMA)] builds on the well-documented porous structure achievable with these copolymers and they are readily available from commercial sources. PS also has a low static dielectric value of⁹ 2.55. The static dielectric values are usually calculated for 60 Hz. The addition of a porous structure should have beneficial effects on the dielectric value as well.

CHAPTER 2

INTRODUCTION AND THEORY

Low- κ Materials

Low- κ materials are those with a dielectric value of less than 3.5. Table 2 has a selection of materials and their dielectric values. The dielectric properties of materials are a function of the density of atoms and bonds present in the material and the polarizability of the material. When addressing the polarizability of a material it is

Dielectric Values for Various Materials^c	
Material	Dielectric Value (κ)
Vacuum	1
Methyl Silsesquioxane (MSQ)	1.6-3.2 ^d
Helium	1.000065
Dry Air	1.00054
Water Vapor (100 °C)	1.00587
Polystyrene	2.55
Silicon Oxide (SiO ₂)	3.9-4.5
Salt	5.9
Silicon Carbide (SiC)	6.52-10.2
Silicon (Si)	11.8

Table 2 A random sampling of dielectric values

commonly broken into three categories. These are the electronic, atomic, and orientational responses of the material. The atomic and orientational responses are the nuclear responses and dominate at low frequencies; however, at frequencies approaching 1 GHz all three responses become important. Minimization of the effects of all three responses is the holy grail of low- κ research. The dielectric constant of any material may be reduced by reducing the materials density. However, it is difficult to reduce the dielectric value below 2.5 with fully dense materials.⁹ One approach to reducing the dielectric value of a material is to introduce porosity.

The impact of porosity on a materials dielectric value can be calculated using the Bruggeman effective medium approximation.¹⁰ Where f_1 is the fraction of material

$$f_1 \left(\frac{k_1 - k_{eff}}{k_1 + 2k_{eff}} \right) + f_2 \left(\frac{k_2 - k_{eff}}{k_2 + 2k_{eff}} \right) = 0 \quad \text{Equation 6}$$

with dielectric value k_1 , and f_2 is the fraction of material k_2 and k_{eff} is the effective dielectric value. This shows that a polystyrene material with 27.5% porosity would have a dielectric value of approximately 2. This is the best value we can hope for in a stable configuration due to percolation of the pores, which ultimately will lead to interconnectivity of the pores.⁹ This occurs with porosities of approximately 30% or greater. This is also a best-case scenario since experimentally it has been shown that moisture contamination of the pores occurs under ambient atmospheric conditions if the pores have not been sealed.⁹

Atomic Force Microscope

The atomic force microscope (AFM) will be used to identify topographical features of our samples. Since our AFM is not operated within a vacuum, we must assume a surface film of moisture is present. However, this absorbed moisture is acknowledged and addressed in the operational software. Both of the AFMs used for this study have similar operations. For both, the scan is a rastering back and forth across the scan area. For the Park Scientific instrument, this rastering is of the sample while the Veeco instrument rasters the tip. Regardless of the sample or tip being moved the area covered is the same, see figure 2. The movement within the area of the scan is accomplished using a piezoelectric tube to either move the sample or scan head. The piezo is normally

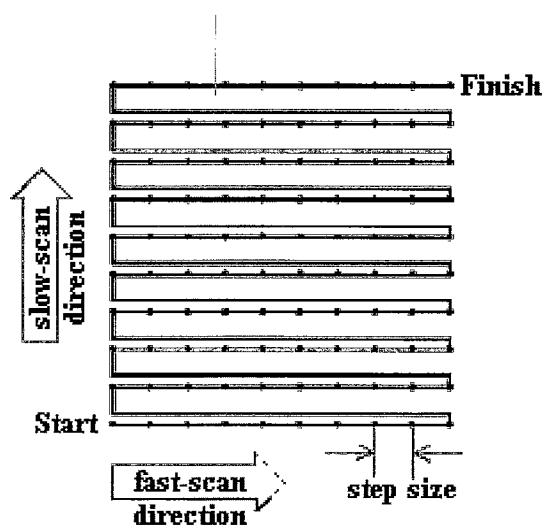


Figure 2 Typical rastering pattern for AFM scan whether the scan head or sample is moved, note that the horizontal lines are separated by a distance equal to the step size along each horizontal line.

constructed from four different piezos bonded together in a flexible tube. Piezoelectric materials will expand or contract when subjected to a potential voltage. The application of a positive voltages to one side of the tube (causing expansion) while a negative voltage is applied to the opposite side (causing compression) will result in movement of the

surface along a particular axis. This system is duplicated for all in plane movement. Movement along the z-axis is a combination of movement within the plane coupled with an out of plane movement that expands or compresses all four piezos, see figure 3. The voltages applied are then recorded and using parameters established during calibration are converted to distances of movement along all three axis. This allows the software

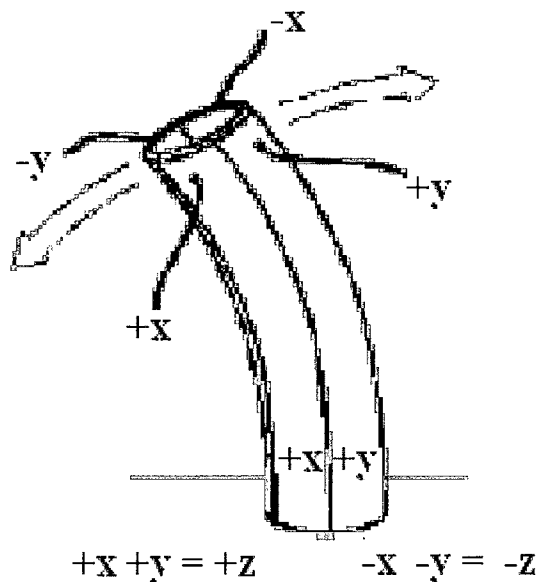


Figure 3 Typical Piezoelectric scanner tube used for sample or tip movement with an AFM.

to return a representative image of the surface. The topographic image provided by the AFM is color enhanced to simulate the approximate height of features detected.

The mechanism for detection of interaction with the surface of the sample is a laser beam reflected from the back of the cantilever into a pair of photo-detectors. The output for the photo-detectors is $A + B$ and $A - B$ where $A + B$ is the sum of the light collected between the two detectors and $A - B$ is the difference.¹¹ As the cantilever moves up and down, the reflected beam is deflected from center between the two detectors see figure 4.

The piezo voltages are adjusted by the control software to force the reflected beam to return to the center of the detector.

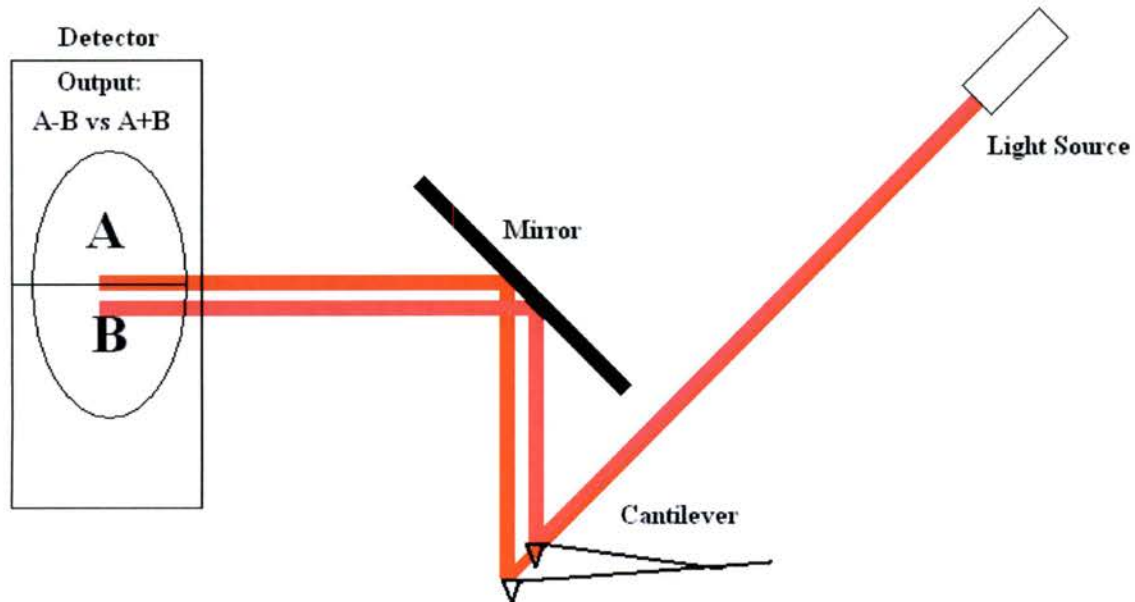


Figure 4 Greatly exaggerated cantilever and beam deflection that will be countered by piezo voltages to return the pink beam to the position of the red beam.

A key element of AFM imaging is the selection of a cantilever and tip type. In part, this is a function of the most likely imaging method to reveal important features. The stiffness of the cantilever used should be appropriate for the sample and imaging method. Tip shape is also important to the resolution of the image since the tip can only provide a trace image of features it is capable of following. A large pyramidal tip structure will be more robust but will fail to detect pits in the surface that have a smaller diameter than it does. Additionally any structure with sidewalls of a greater angle than that of the tip will produce an image of the tip's sidewalls rather than an image of the structure's vertical features (figure 5).

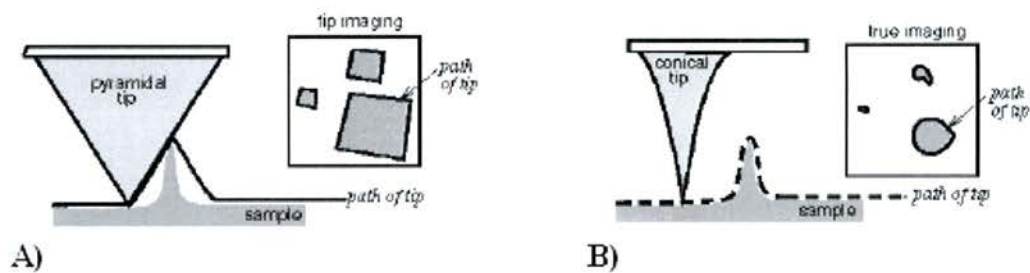


Figure 5 A) A pyramidal tip encountering a structure that is incorrectly reported due to angle of tip sidewall. B) The benefit of using a conical tip is that the same limits from sidewall angle appear, but are greatly reduced by the steeper sidewall construction.

In contact mode, the AFM performs very much like a record player. The tip is held in contact with the surface at a constant force by modification of the voltages applied to the piezoelectric material as determined by the beam deflection. A cantilever with a small force constant has a higher response range when used in contact mode. This type of imaging mode can achieve atomic resolution, with adequate noise isolation. This mode of operation can be destructive to the surface, especially with softer samples. Contact imaging should not be used prior to any other testing of a sample.

The next two modes are tapping and non-contact. Both of these modes of operation utilize an oscillating cantilever. Here the use of a cantilever with a high force constant is desirable. The primary difference in these modes is the amplitude of the oscillations, tapping uses amplitudes of 20-100 nm while non-contact uses amplitudes of less than¹² 10 nm. In tapping mode, the change in the frequency of oscillation brought about by physical contact with the surface is used to create an image of the surface of the sample. In this manner, the information available from a tapping mode scan is very similar to that of the contact mode since both methods employ contact with the surface. The primary difference is that in tapping mode the tip is only in contact with the surface intermittently unlike a contact image where the tip is always on the surface. For non-contact imaging,

the interaction with the surface is not physical contact, but a measurement of the tips interaction with the van der Waals forces of the samples surface, which alter the oscillations of the cantilever. This is the least destructive of AFM imaging methods but it is still not recommended for in process testing of samples. The primary short fall for the non-contact mode of operation is that it is impossible to insure that the image of the surface obtained is the true surface and not also a demonstration of moisture collected on the surface see figure 6.

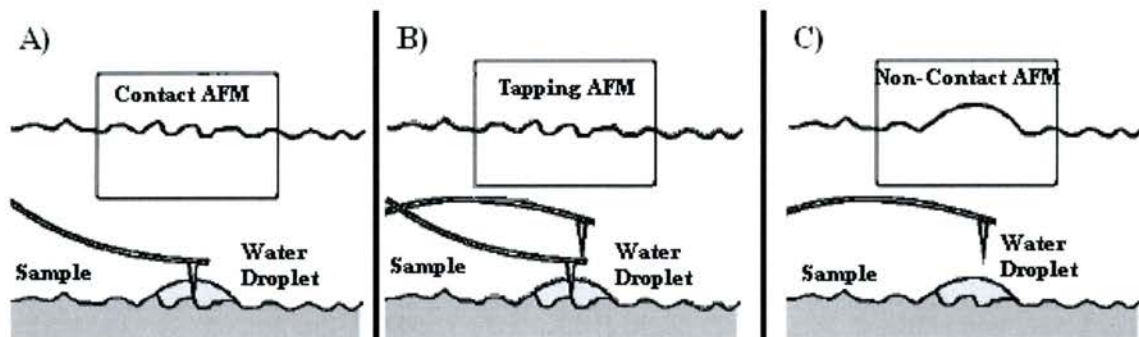


Figure 6 A) Shows an AFM cantilever in constant contact with the surface and the image returned above. B) AFM in tapping mode and hopeful representation of the surface above. C) Failure of non-contact mode of operation for AFM notice the water droplet is reported as part of the surface.

Fourier Transform Infrared Spectroscopy

Fourier Transform Infrared Spectroscopy (FTIR) uses a wide spectrum infrared (IR) source to identify vibrational modes associated with chemical bonds in a substance. Both of our spectrometers operate with wavelengths ranging from of 2.2 μm to 22.2 μm . These values are normally reported as wavenumbers of 4000 cm^{-1} to 400 cm^{-1} although older text's may use the term Kaisers. The FTIR actually measures the absorption of individual wavelengths passing through a substance. This absorption, which is normally reported as percent transmittance, is representative of the energy transferred from the photons to the chemical bonds with complimentary vibrational modes. The energy captured by the chemical bonds causes them to vibrate in a predictable fashion. This vibration may be described as a change in the inter-atomic distances known as stretching or a change in the angle between two bonds known as bending. The different types of bending are scissoring, rocking, wagging, and twisting. Scissoring and rocking are both types of in plane bending, while wagging and twisting are out of plane motions. Of course, any and all of the different vibrations may occur in series or parallel depending on the angle of incidence for the observer. The number of possible vibrations for a polyatomic species is $3N-6$ where N is the number of atoms in the molecule. It is not necessary for the number of vibrational modes detected to equal the maximum number of vibrational modes. As stated earlier, symmetry with respect to the angle of observation may prevent detection. More than one vibrational mode may share similar energies, the intensity of the vibrational mode may not be sufficient for detection or it may be outside the range of the detector.¹³ The significance of each vibration is that every vibration is caused by a specific wavelength. Since the FTIR is designed to compare the intensity of

the source with the intensity transmitted through the sample, it is therefore possible to identify which wavelengths are absorbed by the sample. By comparison of the absorbed wavelengths to known standards of chemical structure it is possible to identify the species present in the sample.^{13,14} It is also possible to identify the structure of the sample by observation of the absorption peaks to identify the bonds present. This ability may make it possible to identify the cross-linking mechanism in our copolymers.

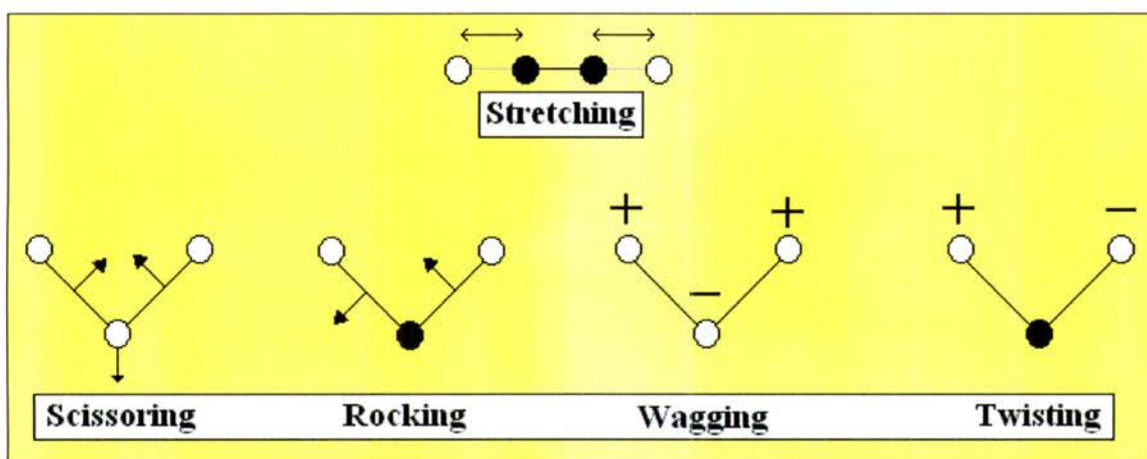


Figure 7 Possible vibrations occurring due to excitation of bonds during FTIR. For simplicity assume all actions are described as changes in the plane of the image. Atoms appearing in black are assumed stationary during the vibration.

Polymers

Polymers are chain like structures composed of repeating units called monomers. For our work, we were concerned with the styrene monomer C_8H_8 and the methyl methacrylate monomer (MMA) $C_5H_8O_2$ (figure 8). Copolymers may be formed with different chain configurations; the random copolymer is just that a random placement of monomers and polymers within the chain, the diblock is a chain that has two sections containing only one monomer type in each section.

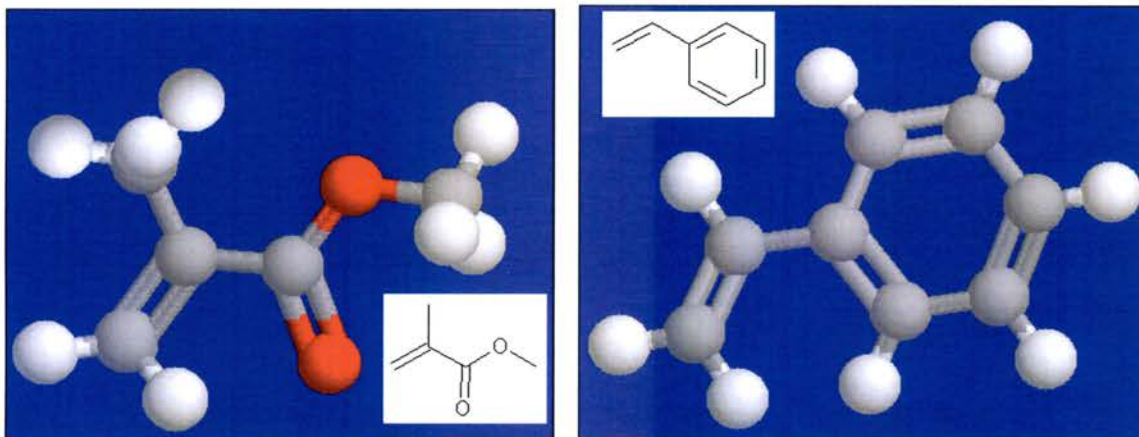


Figure 8 (left) Methyl methacrylate monomer carbon atoms gray, oxygen atoms red; hydrogen white. (right) Styrene monomer.

Polymers are described using not only their chemical formula but also using the weight average molecular weight (M_w), the number average molecular weight (M_n), and the polydispersity index (PDI).

$$M_n = \frac{(\text{total_mass})}{(\#\text{_molecules})} \quad \text{Equation 7}$$

$$M_w = \frac{(\text{mass_polymer_1})}{(\text{total_mass})} \times (\text{mass_polymer_1}) \quad \text{Equation 8}$$

$$PDI = \frac{M_w}{M_n} \quad \text{Equation 9}$$

The use of polymer thin films is a growing field, as is the available information on the behavior of thin film polymers. Polystyrene (PS) and polymethyl methacrylate (PMMA) have vastly different reactions to ultraviolet radiation (UV). PMMA a known negative photo resist will be degraded, when exposed to approximately¹⁵ 3.4 joules/cm² of UV. The effect being that the MMA bonds break making it possible to separate the PMMA from the PS. Exposure of PS to approximately 25 joules/cm² of UV is believed to promote cross-linking within the polymer chains. After exposure to UV the PS exhibits improved resistance to solvents, increased structural strength in the matrix and improved thermal stability. The UV exposure is accomplished as a single action and then the degraded PMMA is removed from the structure by soaking in a PMMA selective solvent such as glacial acetic acid.¹⁶ This also means that the polymers should be handled in the same manner as photo resist because it is subject to the same degradation as photo resist.

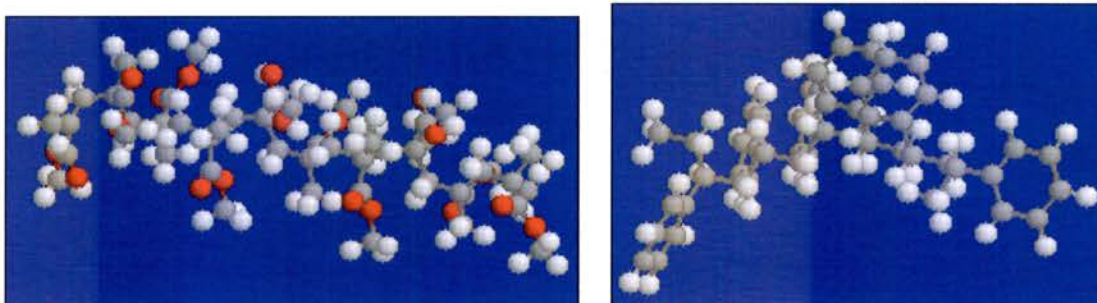


Figure 9 (left) Polymethyl Methacrylate this polymer has ten (10) MMA monomers with the carbon atoms gray, oxygen atoms red; hydrogen white. (right) Polystyrene with six (6) Styrene monomers.

Another important consideration for working with polymers is the glass transition temperature (T_g). For thin films of either PS or PMMA, the T_g is dependent on the film thickness and is different from that of the bulk.¹⁷ If a polymer is below its T_g then the physical structure is glass-like. This same polymer heated above its T_g , but kept below

its melt point, is in a rubbery state. In this temperature regime the α -modes are restricted compared to a liquid state but still have some degrees of freedom.¹⁸ This is the mechanism which allows the hydroxyl (OH) tags on the RCP to migrate to the surface as well as the mechanism that allows the DBC to self assemble. The approximate T_g for our copolymers are listed¹⁹ in table 3. If the annealing process is performed at less than the T_g of both polymers, the final surface will have cracks or splits in it.²⁰

T_g by % PMMA in a copolymer with PS^c						
% PMMA	0	20	40	60	80	100
T_g (°C)	107	103	103	106	109	105

Table 3 Glass transition temperature of thin film copolymers of PS and PMMA by percentage PMMA

Random Copolymer

The random copolymer (RCP) has no definite structure and may vary from copolymer to copolymer within the same production lot. An RCP may have any combination of type **A**, **B** monomers as long as the overall ratio is correct, such as a 50:50 random copolymer may have a structure of **A-B-A-B-B-B-B-A-B-A-A-B-A-A**. Our RCP also has a hydroxyl tag or termination on one end. The purpose of the hydroxyl tag is to facilitate bonding of the RCP to the substrate. When sufficient coverage of the substrate is achieved and the hydroxyl tags are allowed to bond with the substrate via annealing above the T_g the RCP is then forced into an upright brush-like structure.²¹ The use of RCP in this application is not only to promote adhesion but also to provide a non-preferential surface for the application and growth of the diblock.²²⁻²⁶ The presence of the hydroxyl tag requires that application work be done in a low oxygen environment so

that the OH tag of the RCP will bond to the substrate instead of free water or oxygen molecules to which it may be exposed.

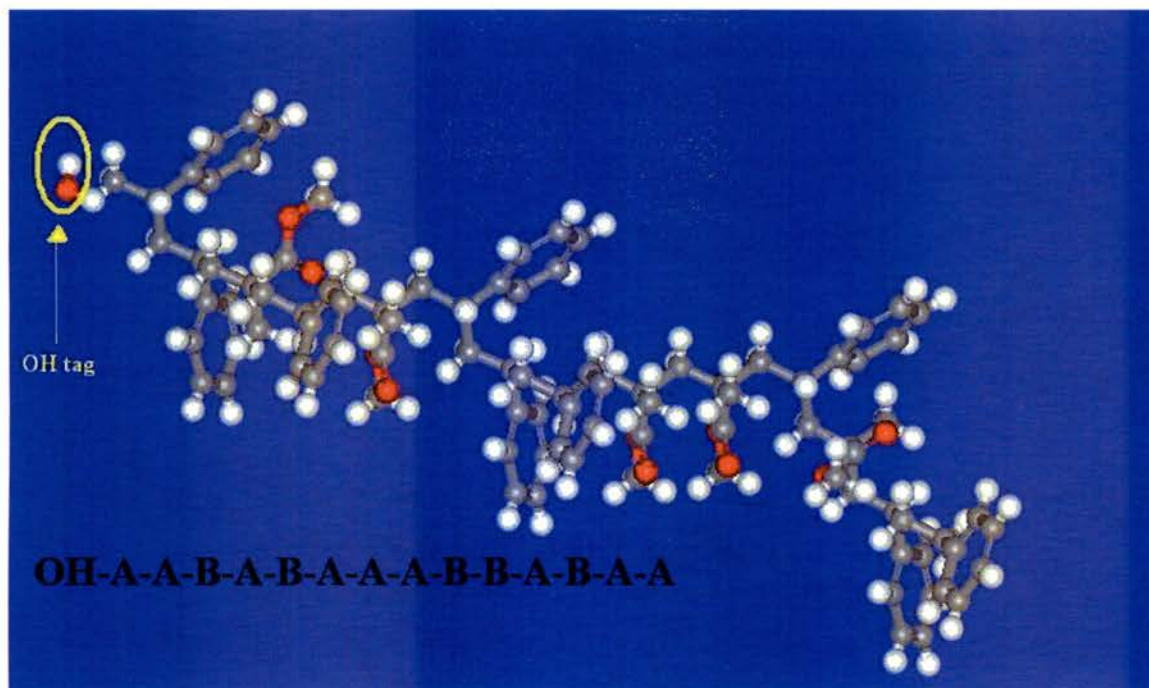


Figure 10 Model of hydroxyl terminated random copolymer of poly(styrene-r-methyl methacrylate) with five (5) MMA monomers (A) and nine (9) styrene monomers (B) notice also the hydroxyl tag upper left end of the copolymer. Gray atoms are carbon, white atoms are hydrogen, and red atoms are oxygen.

Diblock Copolymer

A diblock copolymer (DBC) will have a structure where all like monomers are grouped together so that a DBC may be thought of as a compound of two polymers. A DBC with a 40:60 ratio would look something like **A-A-A-A-B-B-B-B-B-B**.

A DBC of P(S-b-MMA) with a ratio of approximately 50:50 will self-assemble into a lamellar structure after annealing when cast on to a non-preferential surface.^{27,28} If the DBC has a PS ratio greater than 70% the resulting self assembly forms a PS lattice. This lattice is formed during annealing above the T_g when the PMMA forms hexagonal arrays and the PS forms the lattice around the PMMA.²⁹ The size of the PMMA arrays is dictated by both the M_w of the PMMA^{30,31} and by the anneal time. The relationship

between anneal time and array size³² is, approximately t^{-4} . The separation distance of the PMMA arrays is a function of the M_w and of the PS. The presence of the RCP is not mandatory for self-assembly to occur³³ but RCP does aid in bonding of the P(S-b-MMA) as well as promote undirected self-assembly in thinner films.

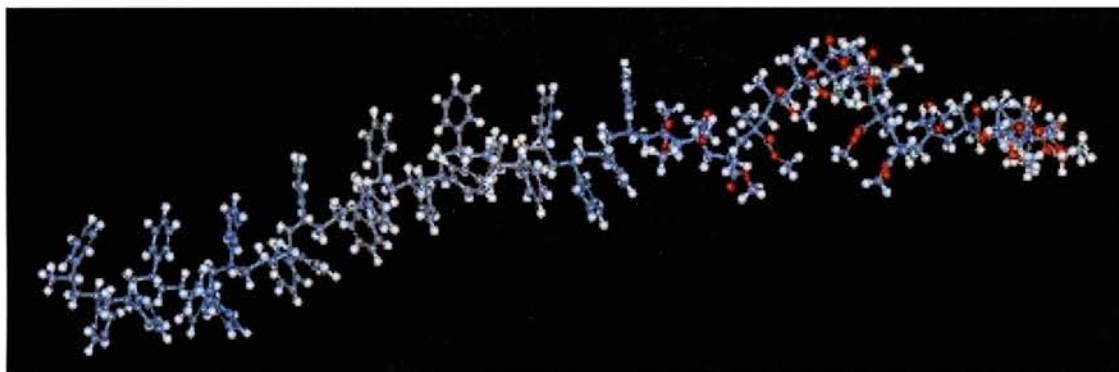


Figure 11 Model of diblock copolymer of polystyrene and polymethyl methacrylate P(S-b-MMA). Gray atoms are carbon, white atoms are hydrogen, and red atoms are oxygen.

Cleaning

To remove a contaminant from the surface of a material you have limited options. The technique of rinsing away contaminants or debris can be optimized by requiring the incident angle to be normal to the surface of the material to be cleaned. This helps to eliminate surface turbulence, which can rob kinetic energy from your rinsing agent and require the solvent to remove the targeted debris or contaminant using chemical action only. The processes currently in use do not rely solely on the transfer of kinetic energy, nor do they rely wholly on the solvation capability of the solvents.^{34,35} Modern cleaning agents are targeted at the surfaces they are meant to clean more than at the agents intended for removal. This process requires a fore knowledge of the chemical interactions and etching rates of the surface to be cleaned. Most modern cleaning techniques work by etching or dissolving a thin layer of the surface to be cleaned. This thin dissolved layer is then held in solution with its trapped debris and contaminants still attached so that they may be rinsed or float away.^{36,37} The biggest demand on the

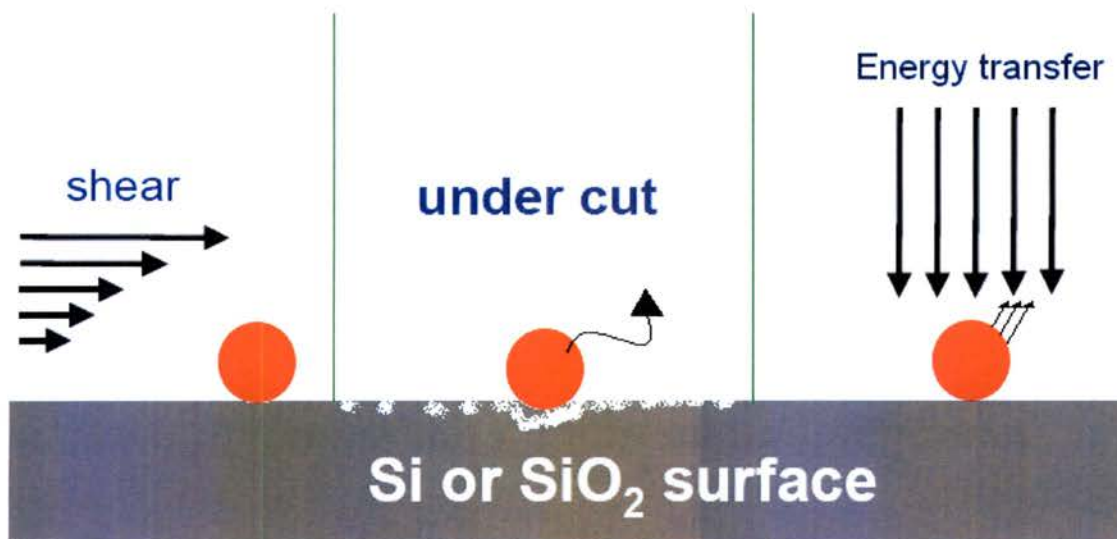


Figure 12 Mechanics of cleaning: (left) inefficiency of parallel flow, (middle) chemical etching, (right) transfer of energy from normal angle of incidence.

cleaning technology though, is to meet the industry requirements or goals as established by the International Technology Roadmap for Semiconductors (ITRS). The 2003 ITRS demands a maximum remaining particle size of $\frac{1}{2}$ the node size. Other demands placed on the cleaning systems by the ITRS are to not increase root means square (RMS) roughness by more than a factor of 100% for an RMS roughness not to exceed 4 Å, and to remove no more than 1 Å of silicon or oxide per cleaning step. The current methods of cleaning Si/SiO₂ wafers are based on the Standard Clean 1 (SC-1) and Standard Clean 2 (SC-2) procedures, which are still considered one of the most effective methods.³⁸

Standard Cleans

Historically the cleaning process was achieved using wet cleans almost exclusively. The current industry standard known as standard cleans (SC-1, SC-2) have another name that identifies their origins RCA-1 and RCA-2 in honor of the company that developed them. The RCA cleans introduced in 1965 were published by Kern and Puotinen in *RCA Review* 1970. SC-1 is a solution of NH₄OH/H₂O₂/H₂O with typical concentrations of 1:1:5 and with optimal efficiency achieved at 70-80 °C. This solution is very effective at removing light organic and metallic contaminants from Si and Si/SiO₂ substrates, the drawbacks being the minor (at the time) etching of underlying structures. SC-2 is a solution of HCl/H₂O₂/H₂O with concentrations of 1:1:6 with an optimal efficiency at 75-80 °C, this solution is effective at removing heavy metal, alkalis and metal hydroxide contaminants from the wafers. Both methods of the standard clean also require rinsing in deionized (DI) water until the resistivity of the water leaving the surface matches that of the water being applied.

These methods, while still in effect, are not completely the same as they were in the 60's and 70's. Both methods have had many optimization procedures explored over the

years in an attempt to meet the current challenges set out by the ITRS. Some of the most obvious ways to improve the efficiencies of the SC techniques is through improved chemical purities, concentration variations, temperature variations, and improvements in the drying techniques. Chemical purity level improvements have been very beneficial with respect to the effectiveness of SC procedures. Continued research into the optimization of chemical concentrations and temperature regimes has added positive effects as well. Perhaps the greatest improvement to the SC techniques has come from improvements to the drying methods. The original drying method, spin-drying, is still in use today with the addition of a second rinse during the spin dry process. With reduction in feature size, water spots have become a problem and new drying techniques have

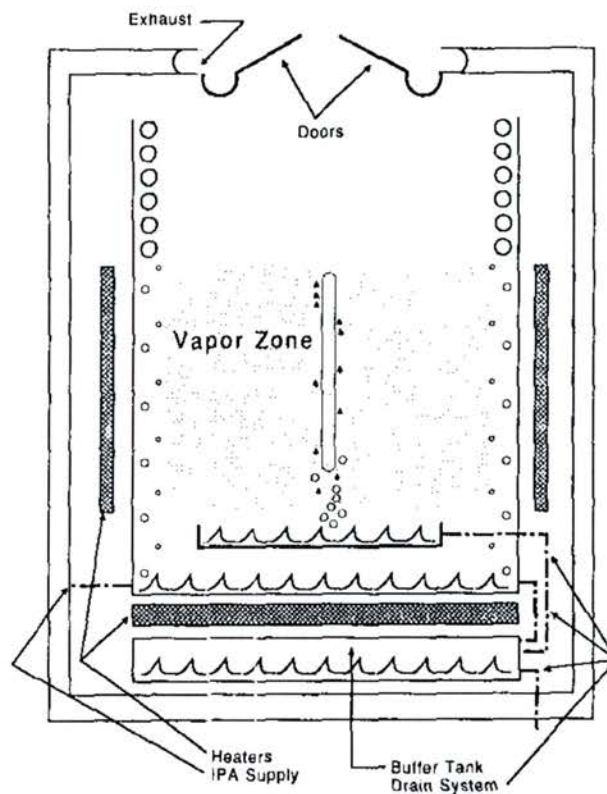


Figure 13 Isopropyl alcohol (IPA) drying tool for improved drying techniques.

helped reduce this problem. Currently the common improvements in drying are the use of isopropyl alcohol (IPA) and Marangoni drying methods. In the IPA method after

either a hot or cold DI rinse the wafer is exposed to a hot isopropyl alcohol vapor that displaces the water allowing it to evaporate. For the Marangoni method the surface of the rinse tank is exposed to vapors of a water soluble liquid which increases the surface tension gradient and causes the water meniscus to contract causing better sheeting of the water across the wafer as it is removed from the tank.^{39,40} Additional improvement in the

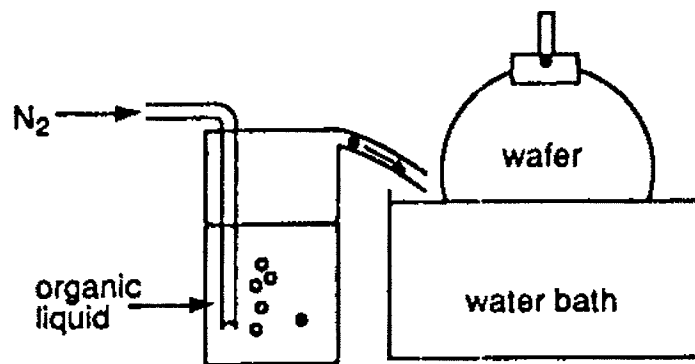


Figure 14 Marangoni drying device improves surface tension helping improve water-sheeting action, providing for a dryer surface.

SC cleans as well as other cleaning techniques have been achieved using constant filtration systems and in situ monitoring of bath conditions.³⁵

Ultrasonic Cleaning

Ultrasonic cleaning utilizes sound in the range of 25-500 kHz to minimize the thickness of the inactive region, which is the solvent surface interface. The use of ultrasound has been found to decrease the thickness of the hydrodynamic boundary layer by approximately two orders of magnitude over that of the same unassisted solvent. The particle removal mechanisms created by the ultrasonic agitation are Eckart streaming (an upward motion in the tank), Schlichting (boundary layer) streaming, cavitation and radiation pressure. The radiation pressure is not a significant factor when the ultrasonics employed are in less than GHz frequencies. The most significant mechanisms are

Schlichting streaming and cavitation. Schlichting streaming because of the reduced boundary layer it creates, allowing smaller particles to become suspended, or receive significant amounts of kinetic energy. While cavitation as shown in figure 15 introduces high-powered gas jets that can free particles from the surface, unfortunately these same jets are capable of damaging the surface of the material.⁴¹

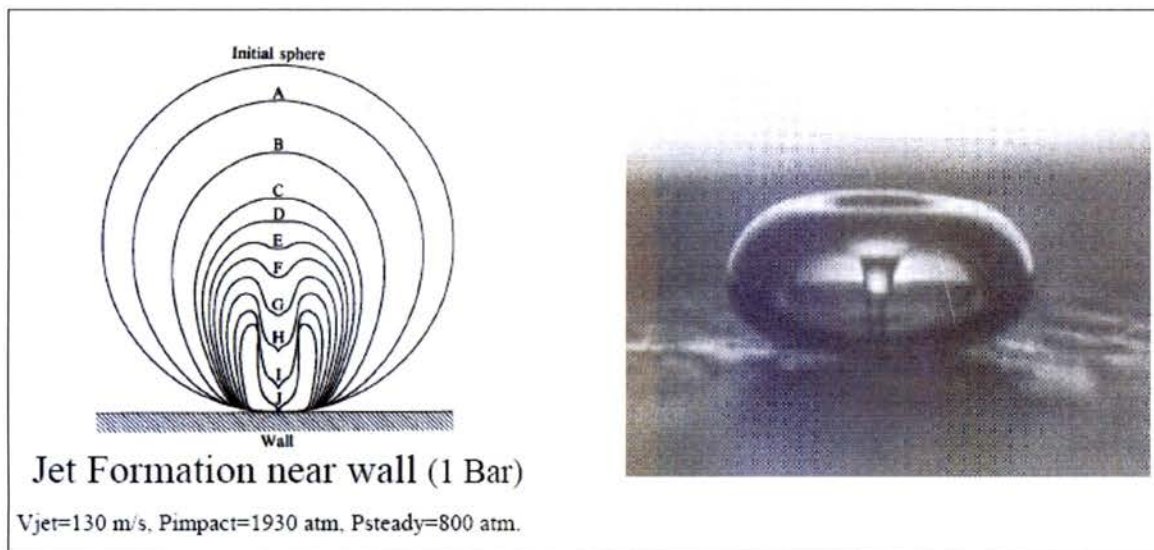


Figure 15 Left to right; drawing of progress from bubble to cavitation, image of air bubble approximately 1 mm in diameter being forced out of suspension and about to rupture.³⁷

CHAPTER 3

PROCEDURES

Consumables List

The following tables provide the specifics for the consumable materials used during the experiments. By maintaining as much consistency as possible in the consumables used, we hoped to eliminate as many variables as possible. The gas and chemical grades are all in-house standards at this time.

Compressed Gas Specifications:					
Compressed Nitrogen (N ₂)		Purity 99.998%			
O ₂	0.11 ppm	CO ₂	< 0.06 ppm	H ₂	< 0.08 ppm
H ₂ O	< 0.08 ppm	CO	0.15 ppm	THC	< 0.1 ppm

Table 4 Compressed Gas Specifications for use with glove box

Chemical Specifications:		
Acetone (C ₃ H ₆ O) (Chromatography grade)	Purity	99.99%
Ammonium hydroxide (NH ₄ OH)	Concentration	29.9%
Hydrogen peroxide (H ₂ O ₂)	Concentration	30%
Hydrochloric acid (HCl)	Concentration	35-38%
Toluene (C ₇ H ₈) (Chromatography grade)	Purity	99.9 %

Table 5 Typical specifications for chemicals used during research

DiBlock Copolymer Specifications: (Polymer Source)			
	P2785-SMMA	P2062-SMMA	P2400-SMMA
Molecular Number (Mn)	39000	74800	67100
Molecular Weight (Mw)	41730	80784	73139
Poly dispersity	1.07	1.08	1.09
PS	Mn 26800	Mn 38000	Mn 46100
PMMA	Mn 12200	Mn 36800	Mn 21000
% PS	68.7179	50.8021	68.7034

Table 6 Diblock copolymers used during research (commercial produced from Polymer source)

Random Copolymer Specifications:		
	P2866-SMMArAn (Polymer Source)	Custom RCP (Craig Hawker, IBM Almaden Research Center)
Molecular Number (Mn)	71300	8000-9000
Molecular Weight (Mw)	132618	Unknown
Poly dispersity	1.86	Unknown
% PS	61.00	55

Table 7 Random copolymers used during the research

Substrate Preparation

The substrates used were amorphous silicon carbide on silicon (SiC), native silicon oxide on silicon (Si) and 1000Å silicon oxide on silicon (SiO₂). The SiC and Si wafers were 200 mm wafers and were donated by Sematech International. The SiO₂ wafers were 150 mm wafers with precut 1.5 cm x 1.5 cm dies. The SiC and Si samples were approximately 1.5 cm x 1.5 cm and separated from the wafer using a diamond scribe to score the reverse side of the wafer along the (100) axis. This scoring creates a cleaving point producing smooth straight edges for the samples. Samples are then scratched in the upper right hand corner in relation to the axis notch on the wafer. This mark is to facilitate alignment and orientation of all samples for Fourier Transform Infrared (FTIR) analysis. The backside of the samples were also marked using the diamond scribe to insure sample identities were maintained see figure 16 a) and b). After separation and

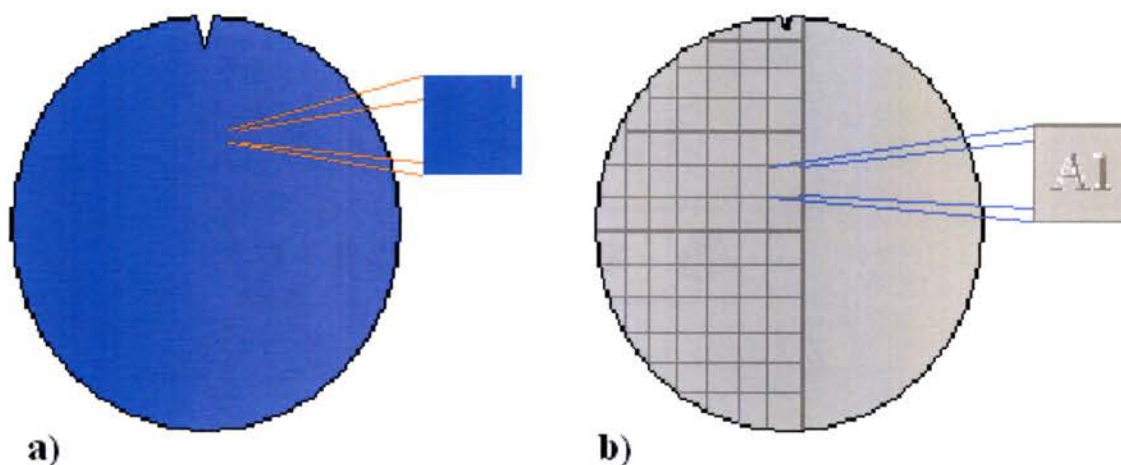


Figure 16 Examples of sample wafers and individual samples. a) Front side of SiC wafer expanded region shows alignment mark for consistent orientation of substrate after separation from the sample wafer. b) Back side of the same wafer as shown in a) with the grid representing scoring before separation of individual sample substrates and the expanded region with sample identifier scratched into the back of sample.

marking of the samples, the samples were cleaned using a 5 min. acetone bath with ultrasonic (5 kHz) agitation. To reduce the possibility of contamination of the samples post cleaning we operated the ultrasonic bath inside the nitrogen-filled glove box where our samples were prepared. In addition, to reduce possible of contamination of the samples we attempted to clean our samples with as little lead-time as possible (on demand cleaning). The samples were removed from the acetone bath immediately following their ultrasonic cleaning. After removal from the acetone the samples were let dry at an angle to prevent drying spots except on the bottom edge. In a nitrogen-filled chamber, the samples are normally dry in under a minute.

Glove Box

The glove box provides a low oxygen, controlled humidity environment for production of samples and solutions. This environmental control is achieved by maintaining a positive pressure of N_2 in the glove box. The internal pressure of the glove box is kept between 1 - 4 inches of H_2O (0.036 – 0.144 psi) above ambient using a compressed N_2 supply. Access to the interior of the glove box is made via an antechamber for introduction and removal of materials to be handled in the nitrogen environment. Work in the glove box was performed with a relative humidity of 7.5% to 10% and an average operating environment of 8% RH.



Figure 17 (left) Glove box with all tools inside and controllers on top. (right) Humidity controller *Nitro watch* and gas supply control *Dual Purge*.

Spin Casting

All thin film samples were spun-cast using a Laurell WS-400A-6npp-Lite single wafer spinner. All of our solutions were applied to the samples in the N₂ environment with a spinner rpm of 1000 and duration of 90 seconds. Approximately 0.5 ml of solution was applied to a typical 1.5 x 1.5 cm substrate.

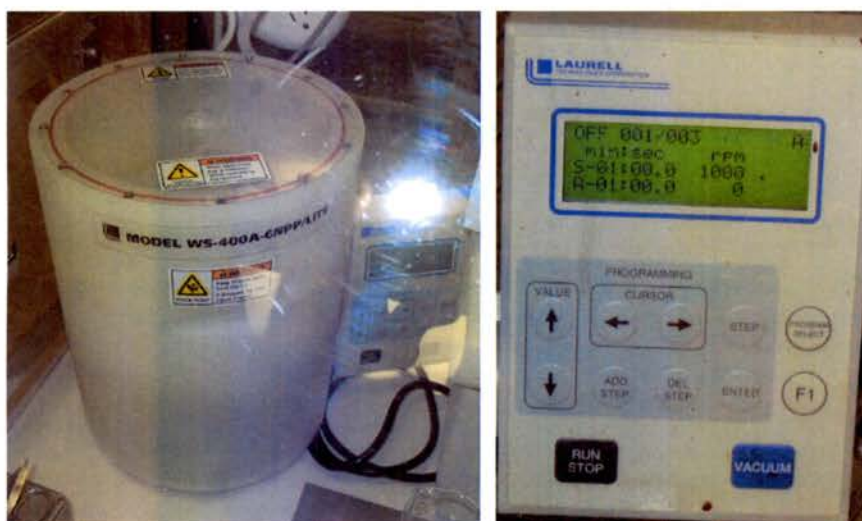


Figure 18 Spinner in glove box and control panel.

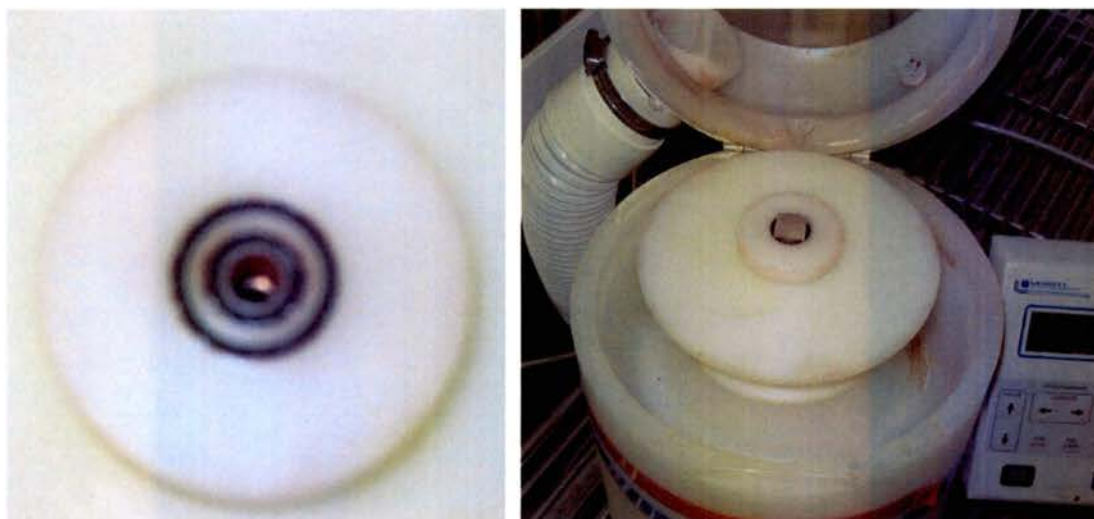


Figure 19 Spinner vacuum chuck without and with sample.

Polymer Preparations

To reduce the possibility of water contamination of the polymers especially the OH terminus all solution bottles were thoroughly washed with soap and water. The solution bottles were then rinsed with acetone and allowed to air dry. After air-drying, the bottles were rinsed with toluene and again allowed to air dry. The sample bottles were then placed in the vacuum oven at 110 °C for 2 hours. The bottles were capped immediately after extraction from the vacuum oven, taken to the glove box, where they were placed in the nitrogen environment. Once the bottles were in the nitrogen environment they were uncapped and allowed to remain in the nitrogen environment for a minimum of 4 hours. The purpose of this step was to remove any moisture the bottles may have collected during extraction from the vacuum oven.

After 4 hours in the glove box, the bottles were capped and removed for empty weighing. Once the empty bottle weights were established, the bottles were returned to the glove box. The bottles were allowed to rest in the glove box until the humidity indicator returned to 8% or less relative humidity (RH). With the humidity again below 8% RH, the weighed bottles were uncapped and polymer was added. The bottles were then recapped and removed from the glove box to be weighed again. The same procedures for return to the glove box were followed once the bottles were weighed. After the environment returned to 8% or less RH, the bottles were again opened and anhydrous toluene was added to create a 1% solution for the diblocks (DBC) and a 0.6% solution for the random copolymers (RCP).

The toluene used was chromatography grade. To remove as much water as possible from the solvent the toluene was distilled using the method described in appendix A.

Random Copolymer

The random copolymer (RCP) we used was P(S-r-MMA) with 55% PS, an OH terminus, and a number average molecular number (M_n) of 8000-9000. The RCP is suspended in a toluene solution of 0.6% by weight. Working in a nitrogen environment with 8% or less RH. The RCP is applied to the substrate using a pipette and spun cast onto recently cleaned substrates. Approximately 0.5 ml of the 0.6% solution is applied to the substrate. Before noticeable drying occurs, the sample is spun at 1000 rpm for 90 seconds. If the sample is not visibly dry at the end of the 90 sec spin then the sample is spun again until dry. These are the procedure for a thin film sample. The thick film samples were prepared using the same technique but were drop cast instead of spin casting and did not receive a rinse after annealing.

After the sample has dried, it is then annealed at 140 °C under vacuum. Post anneal, the samples are allowed to come to room temperature and then the thin film samples are rinsed under a stream of toluene, from a wash bottle, for 20 seconds. The volume of toluene normally consumed during rinsing is 30 to 50 ml. This rinse is to remove any excess RCP that has not bonded to the substrate. The samples are allowed to air dry while resting at an angle of approximately 45°. The angle of 45° helps drive any obvious drying marks to the edges. Ideally, this reduces the effect any residue may have on the final product. Since, we are working in the center of the samples. During the proof of concept and procedural verification work, multiple samples were analyzed using FTIR and AFM. These methods of surface characterization were used both prior to and after the toluene rinse.

Diblock Copolymer

Both the thin and thick film diblock polymers were applied using the same procedure as that described in the RCP procedures with the following exceptions. The samples, post RCP rinse and drying are returned to the nitrogen environment. The glove box humidity is allowed to return to 8% or less RH and the samples are mounted on the spinner. With the samples on the spinner, approximately 0.5 ml of a 1% by weight solution of the DBC is applied via pipette. The samples are spun at 1000 rpm for 60 to 120 seconds.²² Once the samples are dry, they are removed from the nitrogen environment and placed in a vacuum oven for annealing. This is done at 160 °C for 15 minutes to 48 hours depending on desired pore size.^{26,32} Post anneal the samples are rinsed in a stream of toluene from a wash bottle for approximately 20 seconds to remove excess material from the surface. The samples are then exposed to UV for a minimum of 180 seconds. After exposure to UV the samples are soaked in a glacial acetic acid bath for approximately 1 hour to remove the PMMA.^{42,25} During investigation of the self-assembling DBC multiple samples were analyzed using FTIR and AFM both prior to and after the glacial acetic acid bath.



Figure 20 Vacuum or annealing oven. To the left is the vacuum pump, the oven control panel contains power switch, temperature setting, vacuum gauge, and vent/vacuum valves. RCP was annealed at 140 °C and DBCs were annealed at either 160 °C or 180 °C.

Atomic Force Microscopes

Park Scientific (Contact Mode)

Both RCP and DBC samples were studied using the Park Scientific AFM. The Park AFM was used exclusively in contact mode, with an Ultralever[®] ULO6-B tip. Scans in the ranges of 1 μm x 1 μm , 2 μm x 2 μm , 3 μm x 3 μm , and 5 μm x 5 μm were performed.

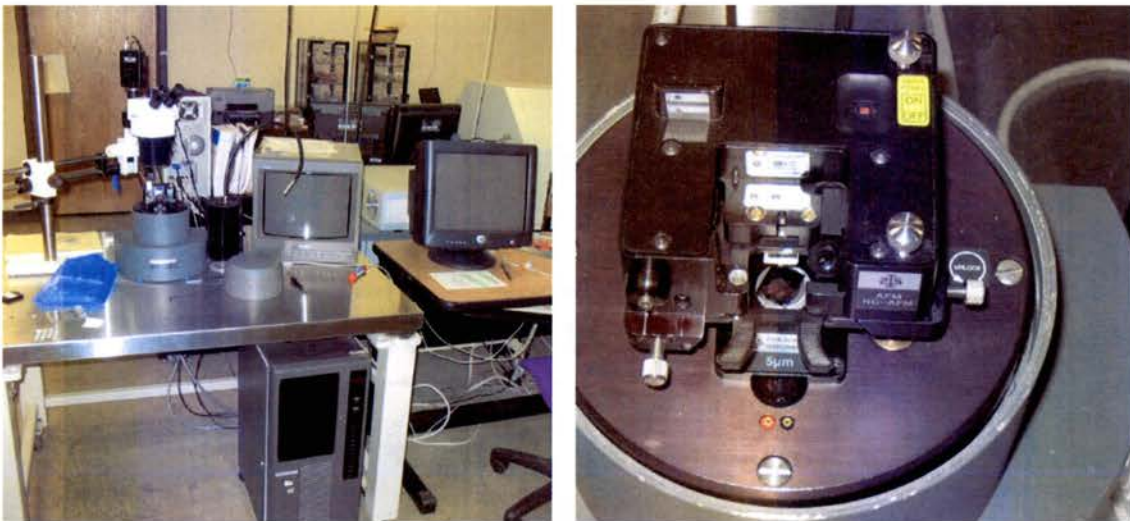


Figure 21 Park Scientific AFM (right) close up of Scanner head with 5 μm scanner installed.

Veeco (Contact and Tapping Modes)

Additional scans of the RCP samples were accomplished using the Veeco nanoscope dimension 3100 nanoscope IV AFM. These additional scans were of 1 μm x 1 μm , 2 μm x 2 μm , and 5 μm x 5 μm areas. Contact mode scans were repeated to test agreement between the different machines and image processing software. Non-contact images were also taken of the RCP samples using the Veeco AFM to verify any RMS roughness variations between the two modes of operation.

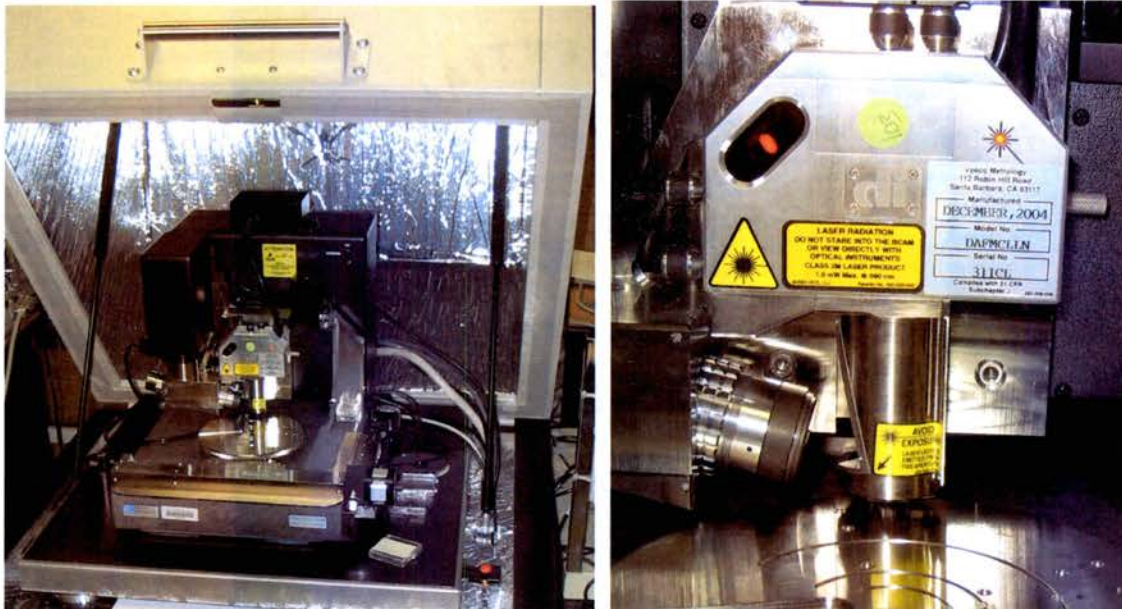


Figure 22 Veeco AFM (left) noise isolation table and hood with scanner head and sample chuck, (right) close up of scanner head and optical focusing system visible to on left side of the scanner head.

Ultrasonic Cleaner

The ultrasonic agitation for the acetone bath was provided using a Branson 1510 Ultrasonic Cleaner. To reduce exposure to possible contaminants the ultrasonic bath was used in the glove box. Because of this placement, we did not use the traditional deionized H₂O for the bath; instead, we filled the reservoir with silicone oil. A 500 ml beaker was then placed in the reservoir and approximately 75 ml of acetone was added to the beaker. The sample substrates were then placed in the acetone bath with a 5 minute ultrasonic agitation. After the ultrasonic agitation was complete, the samples were removed from the acetone and allowed to dry at an angle to minimize the presence of residue in the center of the samples.

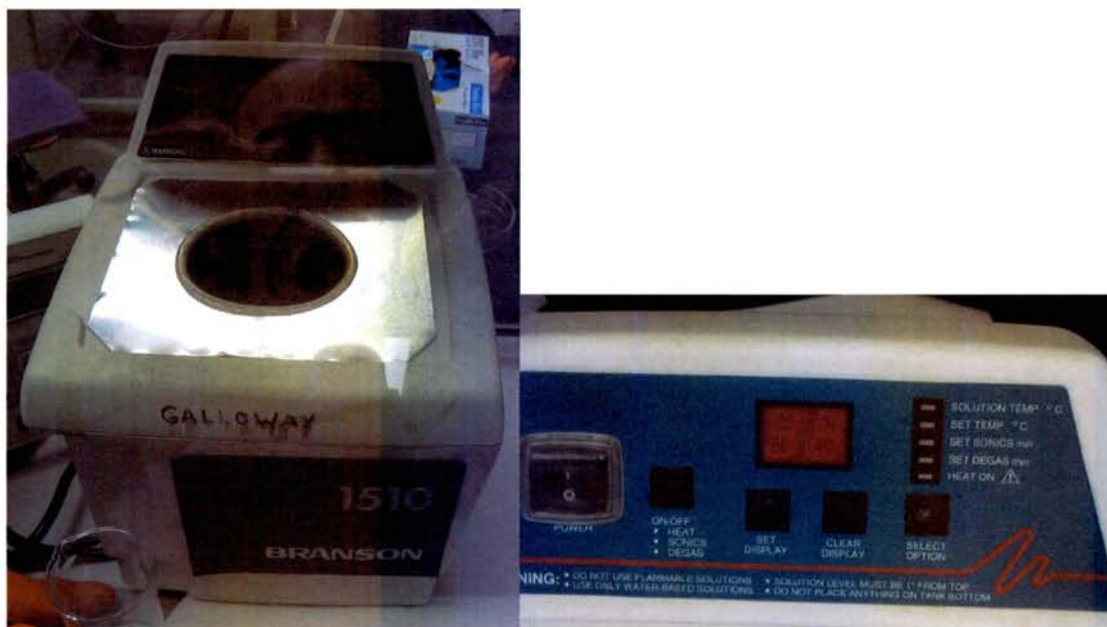


Figure 23 Ultrasonic cleaning system, the reservoir is filled with silicone oil to prevent evaporation and contamination of the nitrogen environment (left) View of control panel for tool (right).

Fourier Transform Infrared Spectroscopes

For fourier transform infrared spectroscopy the basic instrument settings are dictated by the sample. The resolution used for liquid or solid samples is 4 wavenumbers (cm^{-1}) to 8 wavenumbers (cm^{-1}) while gas samples usually require a resolution of 2 wavenumbers (cm^{-1}). The resolution setting is somewhat misleading as it is a complex calculation of the mirror velocity and the spacing of the data points sampled. Therefore, a simpler view may be that a resolution of 4 wavenumbers (cm^{-1}) results in data collection at intervals of approximately 1.928 wavenumbers (cm^{-1}) and a 5 wavenumbers resolution results in data collection approximately every 2.48 wavenumbers. Both of our spectrometers have a variable diameter aperture. The importance of the aperture is to control the incident energy on the detector. A large aperture will increase the signal strength reducing the noise to signal ratio in the scan while a small aperture will improve the resolution of the scan by reducing the quantity of material observed. Finally, the number of scans is the number of data points taken at each frequency or step during the scan. These values are then averaged to reduce the noise to signal ratio, but obviously, this reaches a point of diminishing returns at large numbers.⁴³

Bomem

The Bomem FTIR is controlled using the Bomem software package. The samples observed using the Bomem spectrometer were scanned with a 2.5 mm aperture, a 5 cm^{-1} resolution, and 300 scans. The resulting data was processed using the GRAMS/32 software. The data files were also exported for viewing and analysis using Microsoft Excel ©.

Nicolet 6700

The Nicolet 6700 FTIR is controlled using the Omnic software version 7.1a. All of our spectra were taken using the TGS-MIR room temperature detector. All scans were performed using the default transmission mode with a 2.5 mm aperture, a 4 cm^{-1} resolution and 100 scans. After initial viewing the spectra were exported to Microsoft Excel © for additional analysis.

Ultraviolet Radiation

The samples are exposed to Ultraviolet light after the DBC is annealed and rinsed. Two different apparatus were used during the course of the experiments. These were a FOTO/UV® 300 Transilluminator - which provided wavelengths of 325 nm and a photo resist lamp that yielded wavelengths of approximately 365 nm. In both cases, the samples were exposed to the UV radiation for at least 180 seconds. This is done to promote the cross-linking of the PS and to degrade the PMMA.¹⁶

Cleaning Study

For the cleaning study we wished to compare the effects and efficiency of our 5 minute acetone bath with ultrasonic agitation to the results produced using the industry standard of standard clean 1 (SC-1) and standard clean 2 (SC-2). The first part of the procedure was to establish if our methods of observation were sufficient to detect contamination prior to cleaning. For this purpose, we marked two samples of SiC as described in substrate preparation and established a baseline value for each specimen using FTIR. The FTIR used was a Nicolet 6700 FTIR with Omnic 7.1a software. Once a baseline spectrum was available, one sample was deliberately contaminated with facial oil or sebum an organic compound with an approximate composition of 25% wax monoesters $\approx (C_{21}H_{40}O_4)$, less than 35% triglycerides $\approx (C_6H_8O_6)$, less than 13% free fatty acids $\approx (C_{18}H_{34}O_2)$, and 15% squalene⁴⁴ $\approx (C_{30}H_{24})$. The two samples were again viewed using FTIR and compared to the baseline spectra. The successfully contaminated sample was then cleaned using a 5 minute bath in acetone with ultrasonic agitation. A third FTIR spectrum for each sample was taken and compared to the baseline and contaminated spectra.

A second area of concern when using the FTIR was how sensitive is the instrument or spectra to misalignment of the sample orientation? To address this question we used a sample of amorphous SiC on Si with an RCP brush present on the surface. By using a sample with an RCP brush present, we can also check for shifts in the RCP spectra due to sample orientation.

The third area of concern, was can we detect chemical changes to the substrates that are specific to one or all of the cleaning techniques. For this study, we chose as our base

line reference an as received sample. The as received sample is one removed from a wafer that has been stored in its shipping container outside of a clean room environment. The samples are marked for identification purposes as described in substrate preparation. The study was performed using samples of 1000Å SiO₂ on Si, amorphous SiC on Si and amorphous SiCN on Si. Four samples of each surface were prepared for the study. All four samples of each surface were subjected to FTIR before any action other than the scribing of marks was performed. With baseline spectra for each of the four samples for each material, we proceeded to clean our samples. The as received samples were left untouched except for being stored under the same conditions as the cleaned samples. The acetone bath samples received a 5 minute acetone bath with ultrasonic agitation. The SC-1 sample was cleaned using a solution of deionized H₂O (minimum resistivity of 13.9 MΩ cm): H₂O₂ (30%): and NH₄OH (29.9%) in a 5:1:1 concentration. The SC-1&2 samples were cleaned using the same SC-1 bath as the SC-1 samples and after rinsing were cleaned using an SC-2 solution of 6 parts deionized H₂O: 1 part HCL (35-38%) and 1 part H₂O₂ (30%). After the final rinse both the SC-1 samples and the SC-1 & SC-2 samples were subjected to a 4 hour bake at 110°C and 25 inches Hg of vacuum to insure all volatiles had been removed. From this point forward, all samples were stored under vacuum except during characterization. FTIR spectra were taken for each sample post clean this includes the as received sample, which was used to detect any drift in the apparatus. After FTIR, the samples were imaged using a Veeco nanoscope dimension 3100 nanoscope IV AFM in non-contact mode and using an Ultralever tip, to determine any change in the RMS roughness. Scan sizes of 1 μm² and 5 μm² were used to determine RMS values.

CHAPTER 4

RESULTS

The results are broken into four categories, first documentation of the fourier transform infrared spectroscopy's (FTIR's) ability to detect monolayer thicknesses of a random copolymer (RCP) and to detect possible contamination of a sample as well as its sensitivity to sample orientation and to background or reference scan aging. Second, the results of our cleaning study for the different substrates of interest: SiO₂ on Si, amorphous SiC on Si, and amorphous SiCN on Si. Third, the results of the tests used during optimization of the RCP casting and annealing process. Finally, the results of the diblock copolymer (DBC) applications we performed.

Fourier Transform Infrared (FTIR) Qualification

The results of our qualification test for the Bomem FTIR and detection of RCP on the surface of a sample showed it was possible to detect both an unrinsed thick film, and a thin film after anneal and rinse. The thick film spectrum was compared to the substrate spectrum to reveal the presence of peaks representative of both polystyrene (PS) at 3030 cm⁻¹ and polymethyl methacrylate (PMMA) at 1729 cm⁻¹ and 2970 cm⁻¹. These same peaks are present for the thin film or RCP brush although the intensity of the peaks is significantly reduced with the RCP brush. However, this is to be expected with a much thinner film. Regrettably, the presence of an additional DBC is not so easily detected due to the presence of the RCP, composed of the same polymers. FTIR is not a quantitative

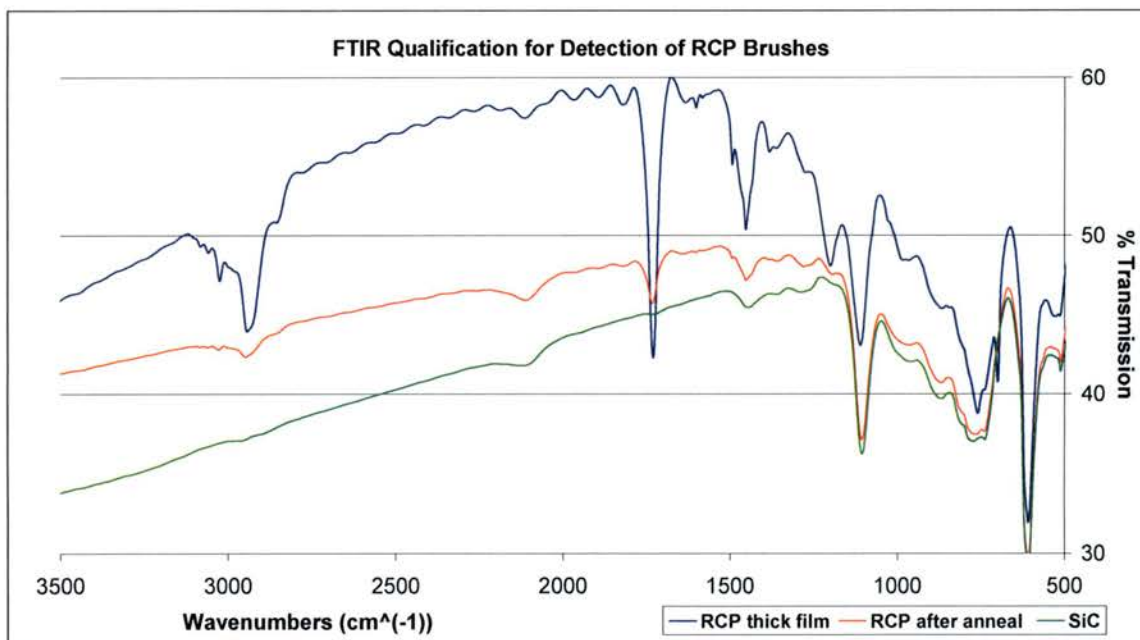


Figure 24 Comparison of FTIR spectra from the Bomem instrument for a thick film of RCP on SiC (blue), an annealed and rinsed RCP thin film or RCP brush on SiC (red) and SiC (green). Note the peaks at 1729 cm⁻¹ and 2970 cm⁻¹ indicative of PMMA and 3030 cm⁻¹ for PS.

measurement device and it is not possible to quantify an increase in the presence of either polymer. It is conceivable, although unproven in our work, that after selective removal of the PMMA a porous DBC would have better defined PS peaks.

Figures 25 & 26 show the results of the scans taken to test detection capabilities after contamination. These and all subsequent qualification scan were taken using the Nicolet 6700 FTIR. The SiC samples were deliberately contaminated with facial oil or sebum to evaluate both the efficiency of our FTIR scan parameters at detecting the contamination and to evaluate the acetone bath effectiveness. The post clean sample has a decrease in transmittance of 0.7%, which may be attributed to both rated instrument stability of 0.5%, alignment of the inscribed sample identifier on the back of the sample, or aging of the background scan. Since the decrease in transmission was not detected in any subsequent testing, we believe this result to be anomalous.

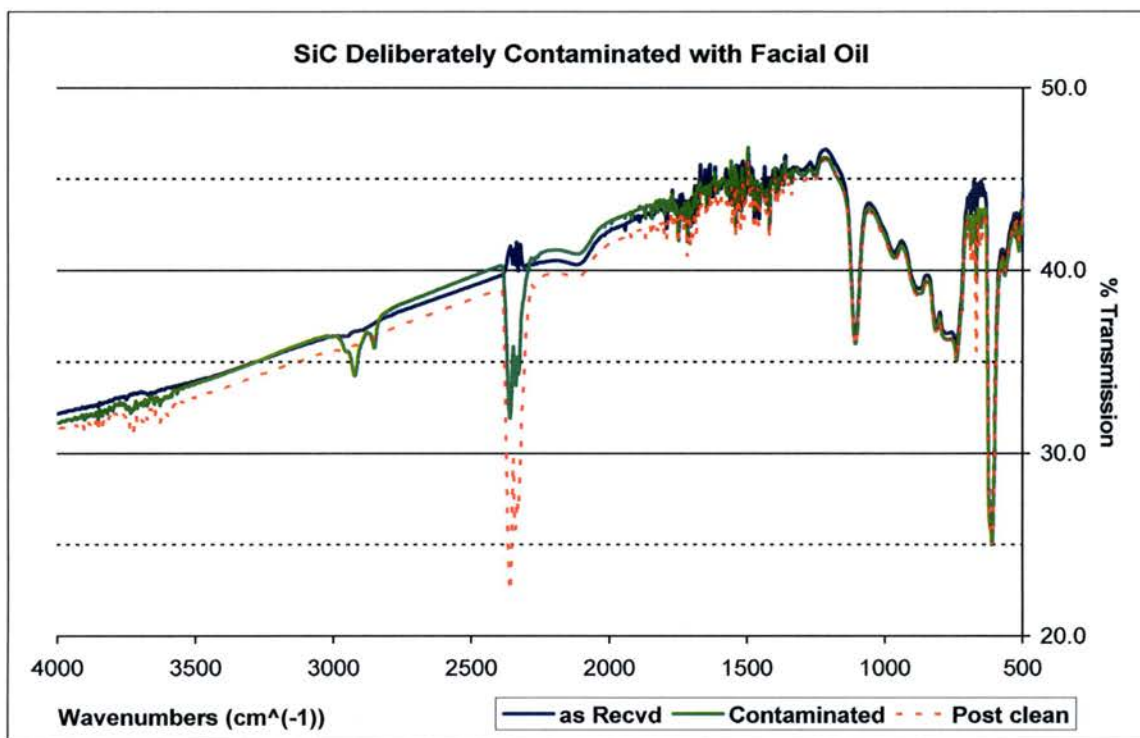


Figure 25 FTIR scan of deliberately contaminated SiC sample before contamination (blue) after contamination (green) and post clean (orange).

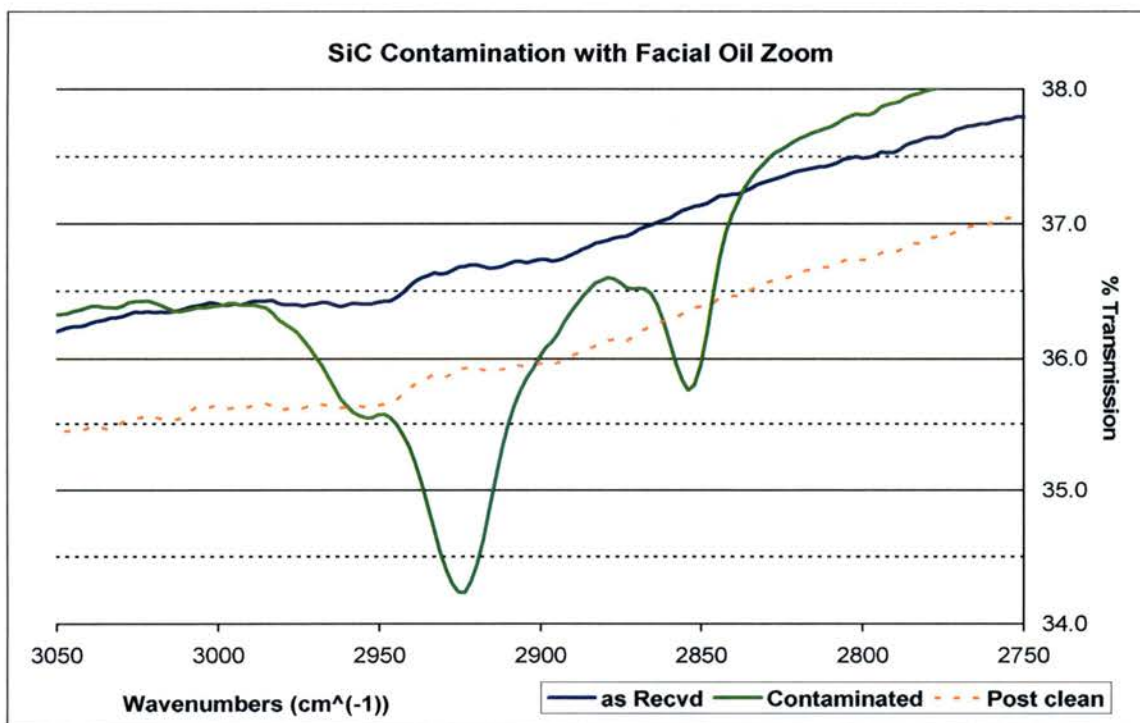


Figure 26 Zoom of FTIR scan 2750 cm^{-1} – 3050 cm^{-1} wavenumbers. The decrease in percent transmission after cleaning is believed to be an instrument anomaly

Qualification of FTIR sensitivity to sample orientation is necessary to insure that all results are due only to the materials of interest. In figures 27 thru 29 below the effect of sample orientation is verified. This test was performed on SiC samples with an RCP brush already present on the surface. We found the greatest variation in the percent transmission to occur at a sample orientation of 90°. The variation is approximately 1.1% in the regions of interest for the detection of PS (2970 cm^{-1}) and PMMA (3030 cm^{-1}) and less than 3% globally. As can be seen below there is no change in the peak at 2100 cm^{-1} to 2150 cm^{-1} , which is representative of SiC. It is also possible to see that orientation has no effect on the Si peaks at 609 cm^{-1} and 1100 cm^{-1} . Sample orientation also has no adverse effects on the weak peak at approximately 2960 cm^{-1} that represents PMMA after the excess unbonded RCP material is removed.

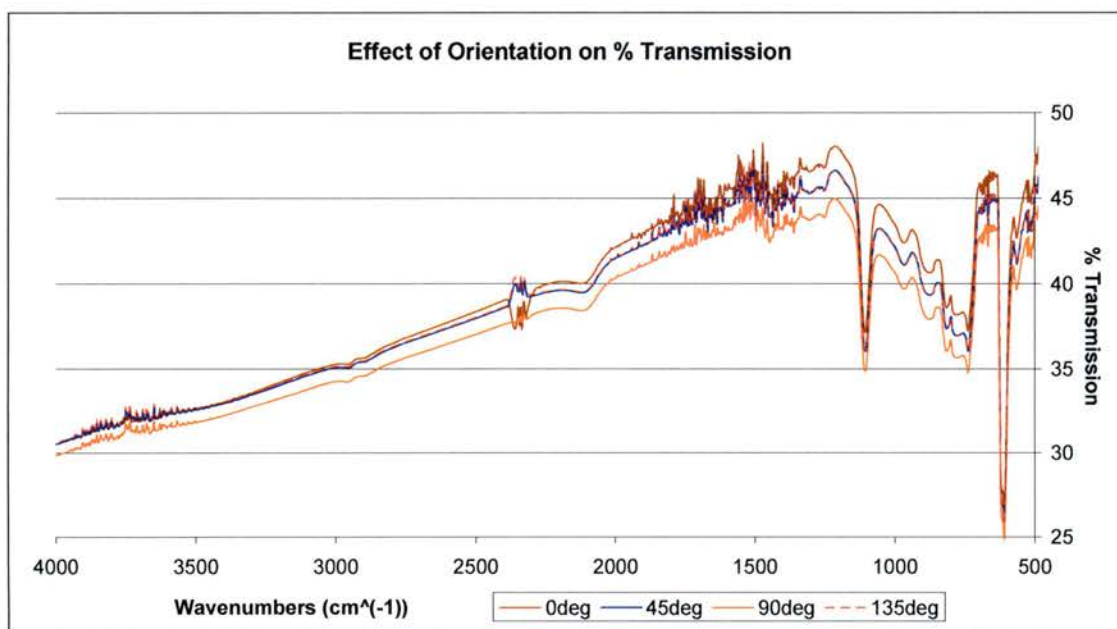


Figure 27 Sample is RCP on SiC orientations of 0°, 45°, 90°, and 135°. Orientation of the sample has no apparent effect on the intensity or position of peaks, only on the overall percent transmission with approximately 3% variation globally.

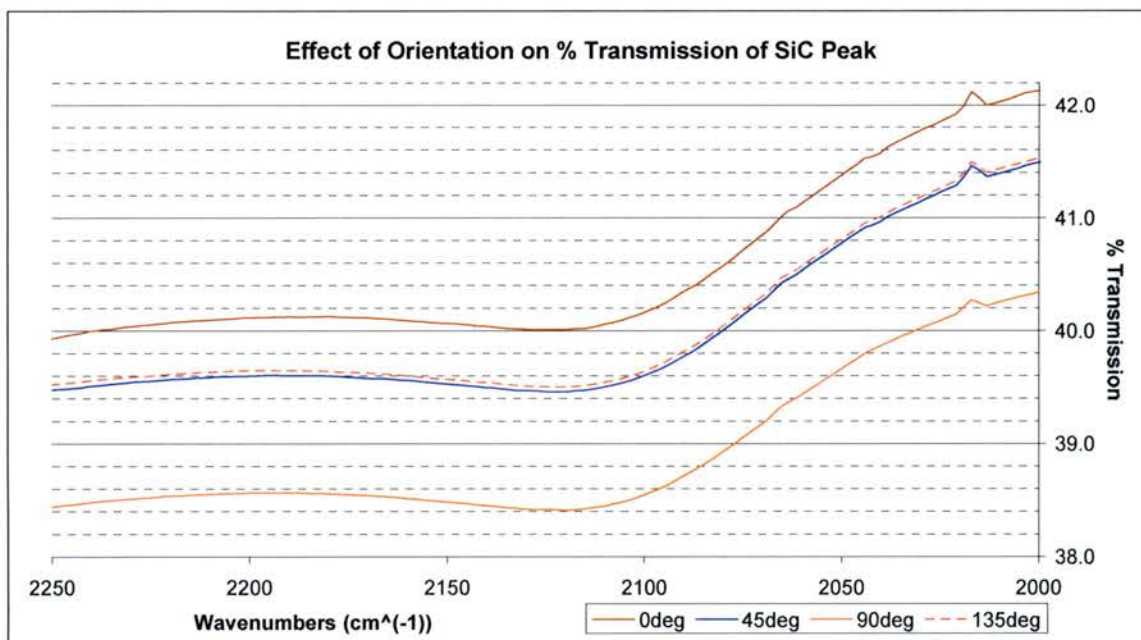


Figure 28 A deviation of 90° creates the largest variation in transmittance. Here the maximum deviation from orientation is $\approx 1.1\%$.

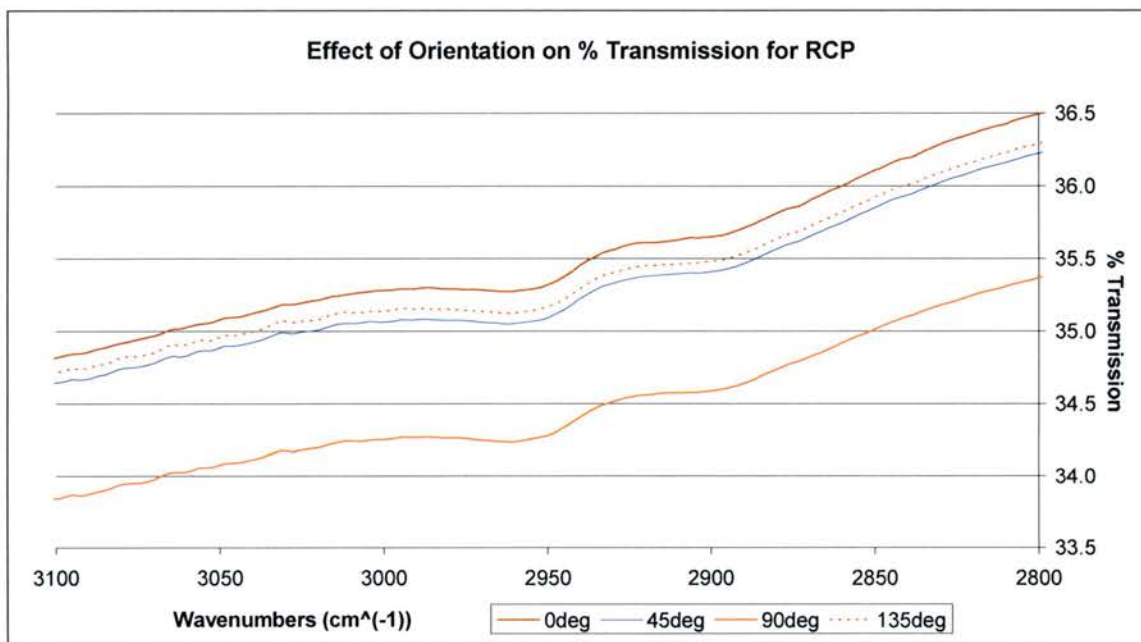


Figure 29 Changing the orientation of the substrate has no adverse effects on the significance of the peaks representing the RCP brushes.

It is also necessary to demonstrate the effects of the background scan aging on the resulting FTIR scans. The scan in figure 30 shows variation due to aging of the background scan and minor variations in the amount of time allotted for the purge after

the sample was placed into the instrument. The scan shown below shows less than a 0.2% variation over the course of 85 minutes from the time of the background scan. The only outstanding variation with time is in the peak that represents the detector window between 2240 cm^{-1} and 2400 cm^{-1} . This is due to the large absorption in the background spectrum by the detector window, so that small variations over time become very pronounced in this region.

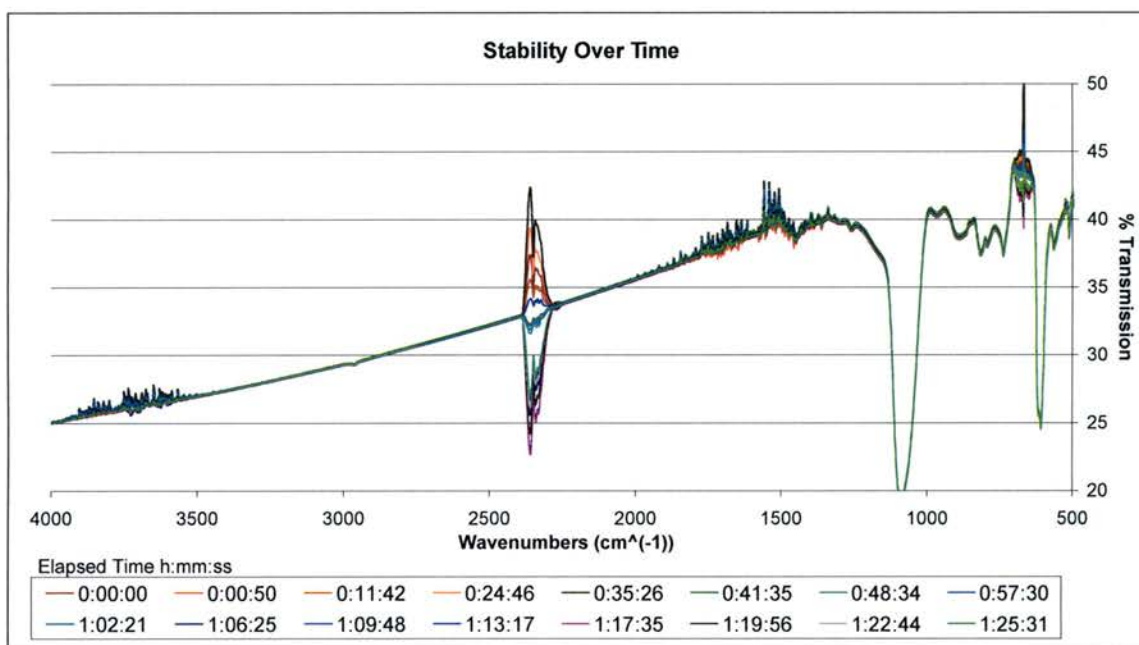


Figure 30 Variation in percent transmittance is less than 0.2% due to aging of the background scan. The legend shows the age of the background scan in an – hour: minute: second format.

Cleaning study

During our investigation, we looked at the effectiveness and impact of different cleaning methods. This was done using both fourier transform infrared spectroscopy (FTIR) and atomic force microscopy (AFM). FTIR was used to identify any major chemical changes in the post clean surface. The AFM was used to evaluate RMS surface roughness before and after the different cleaning procedures to see if any of the procedures would have any adverse effects with respect to surface roughness. A second purpose for RMS roughness characterization was to provide a baseline measurement for interpretation of RMS roughness values for the RCP brushes.

FTIR work for the cleaning study was performed exclusively on the Nicolet 6700 FTIR using 100 scans with a 4 cm^{-1} resolution. For all of the FTIR spectra, the following descriptors were used to identify each sample: for our reference sample, as received (As Rcvd) although as stored might have been more accurate, 5 minute acetone bath with ultrasonic agitation (Acetone), SC-1 cleaning⁴⁵ (SC1), SC-1 followed by SC-2 (SC1&2). In addition, each spectra legend has a suffix attached to the identifier for placement in the test procedure. These suffixes are -BL – for base line the spectra before any action was taken, -1 – first scan after cleaning, -2 – second scan after cleaning.

Using FTIR, we did not detect any significant change to the surface chemistry of our samples from any of our three cleaning methods. This negative result was not immediately apparent. The following spectra for the different cleaning methods on the different substrates have overall variations in the percentage of transmission of approximately 1% per substrate. The initial analysis of these spectra did not include the baseline spectra for each sample and appeared to indicate a relationship between the

cleaning method and the percent transmission. The addition of the baseline spectrum for each individual sample, to the final spectra showed that the variation detected is not an effect of the cleaning method. The variations are caused either by inconsistencies in the substrate wafers we were using, or by the identifying marks inscribed on the back of the samples. If the later is responsible for the variation then it demonstrates an improved repeatability in sample placement from a modified sample holder. The minor changes we did detect were extremely weak peaks throughout the SiO₂ spectra that vanished after cleaning. We also detected very weak peaks in the SiC spectra that appeared after each of the cleans. We attribute these changes to the removal of atmospheric contaminants present before the samples were cleaned. This is based on visual observations of AFM test structures stored under similar conditions that have 3.5-4 μm debris particles with a density of approximately 1 per 14000 μm².

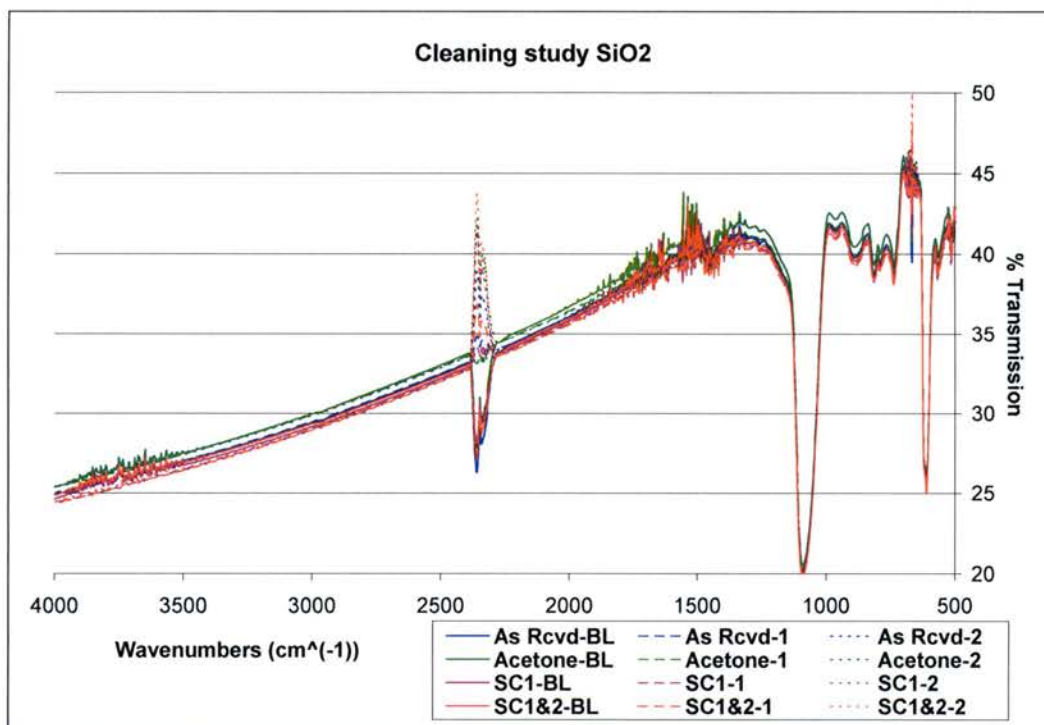


Figure 31 Comparison of cleaning methods for SiO₂ an uncleaned sample ((blue), acetone bath (green), SC-1 (purple) and SC-1 and SC-2 (red) there is no noticeable change from the base line scan.

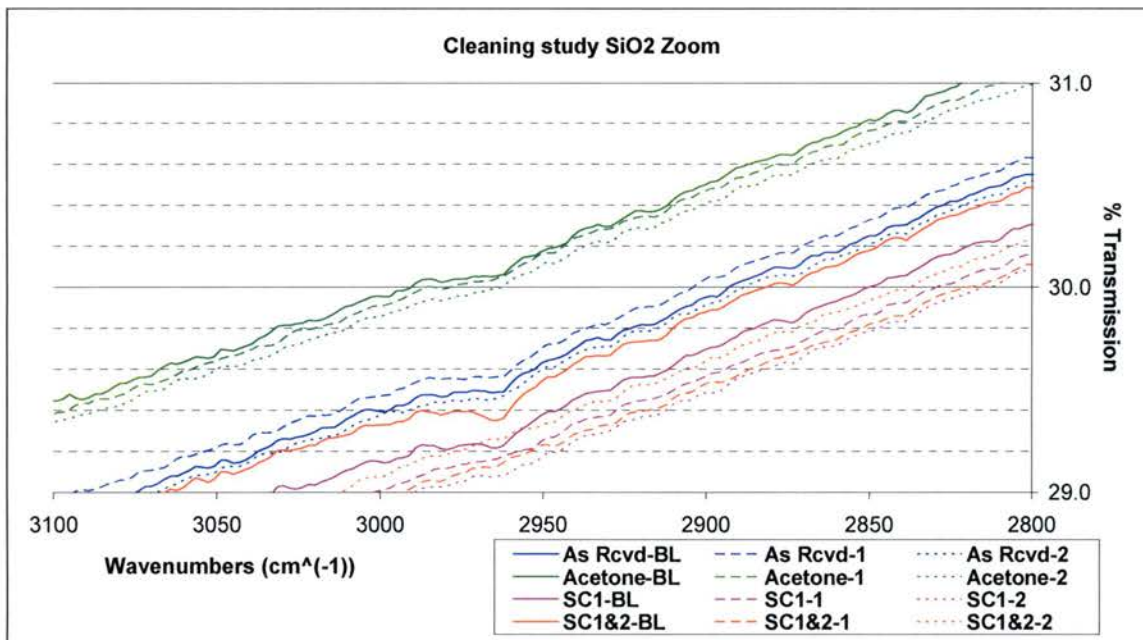


Figure 32 As Rcvd, Acetone and SC1&2 all have variation of less than 0.2% SC-1 has a variation of 0.4% but this is not indicative of any change to the transmission rate for the substrate due to cleaning. The greatest variation is seen in the transition to different locations in the wafer, this variation approaches 1%.

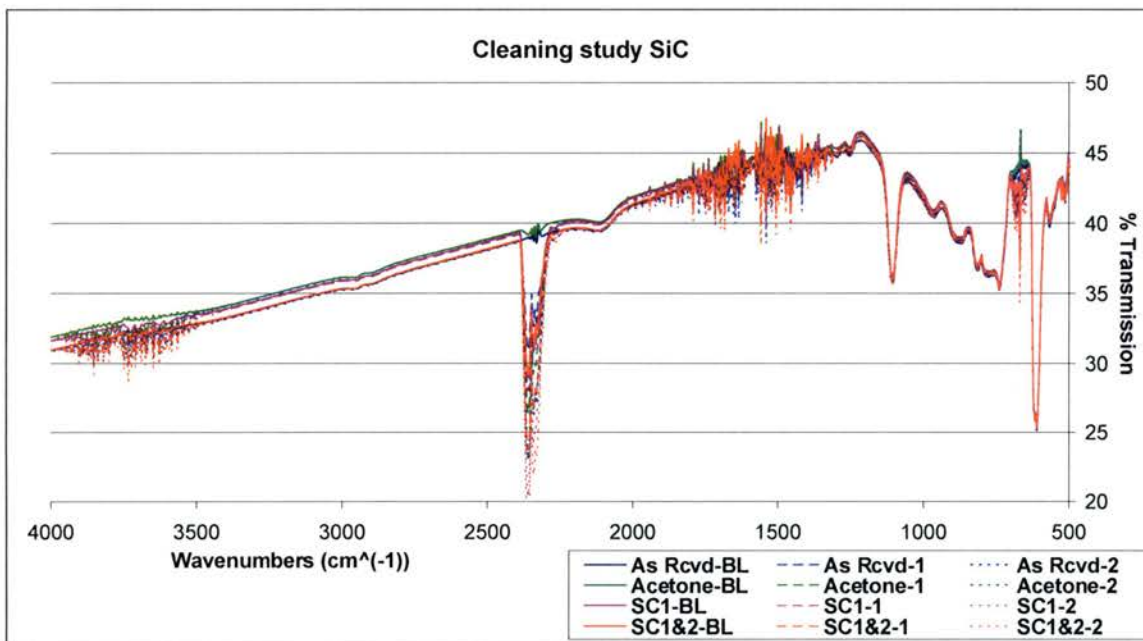


Figure 33 Comparison of cleaning methods for SiC an uncleaned sample ((blue), Acetone bath (green), SC-1 (purple) and SC-1 and SC-2 (red) there is no noticeable change from the base line scan.

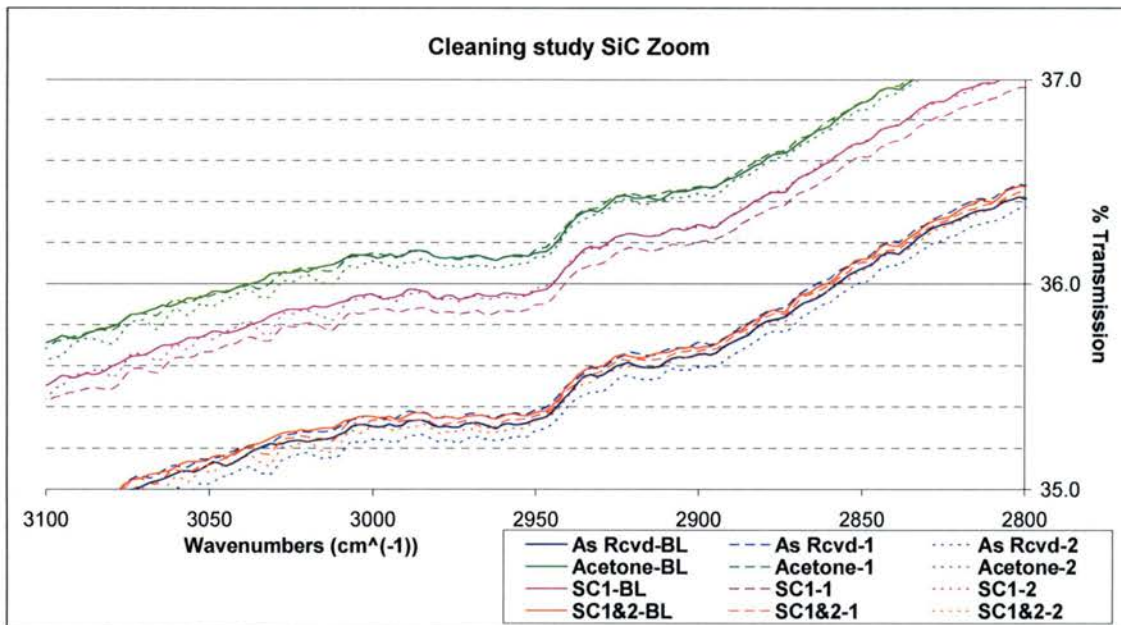


Figure 34 As Rcvd, Acetone, SC1 and SC1&2 all have variation of less than 0.2 this is not indicative of any change to the transmission rate for the substrate due to cleaning. The greatest variation is seen in the transition to different locations in the wafer, this variation approaches 1%.

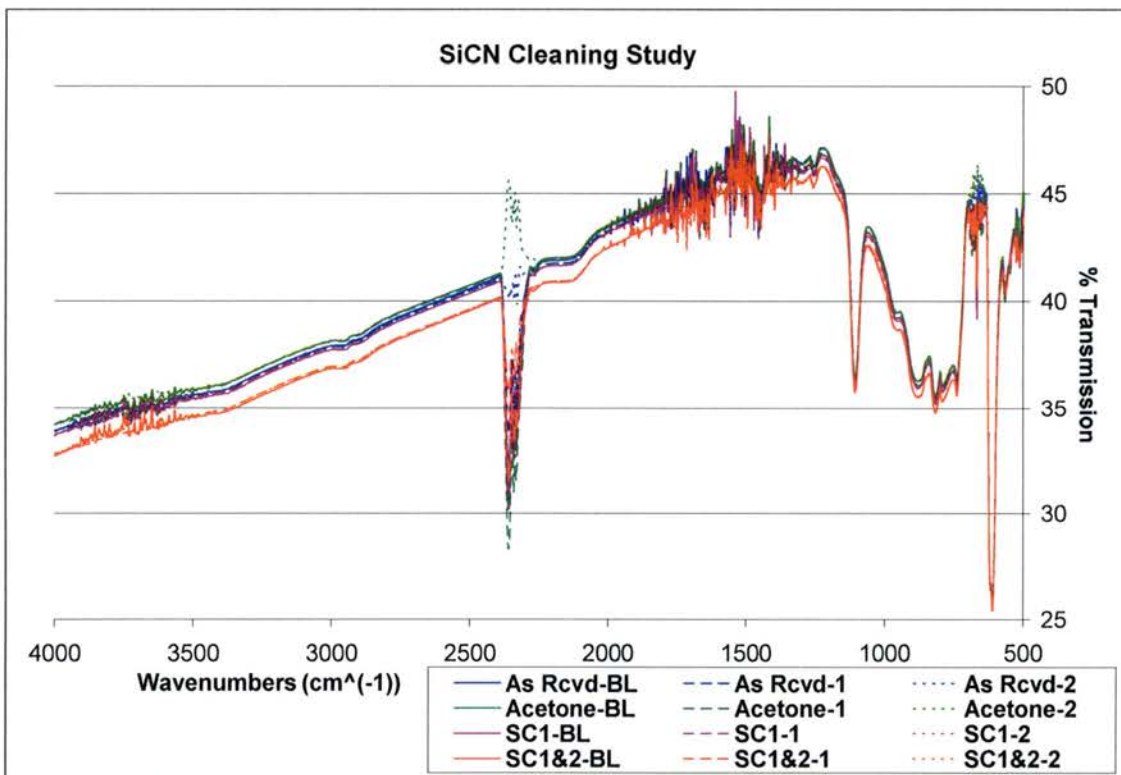


Figure 35 Comparison of cleaning methods for SiCN an uncleaned sample ((blue), Acetone bath (green), SC-1 (purple) and SC-1 and SC-2 (red) there is no noticeable change from the base line scan.

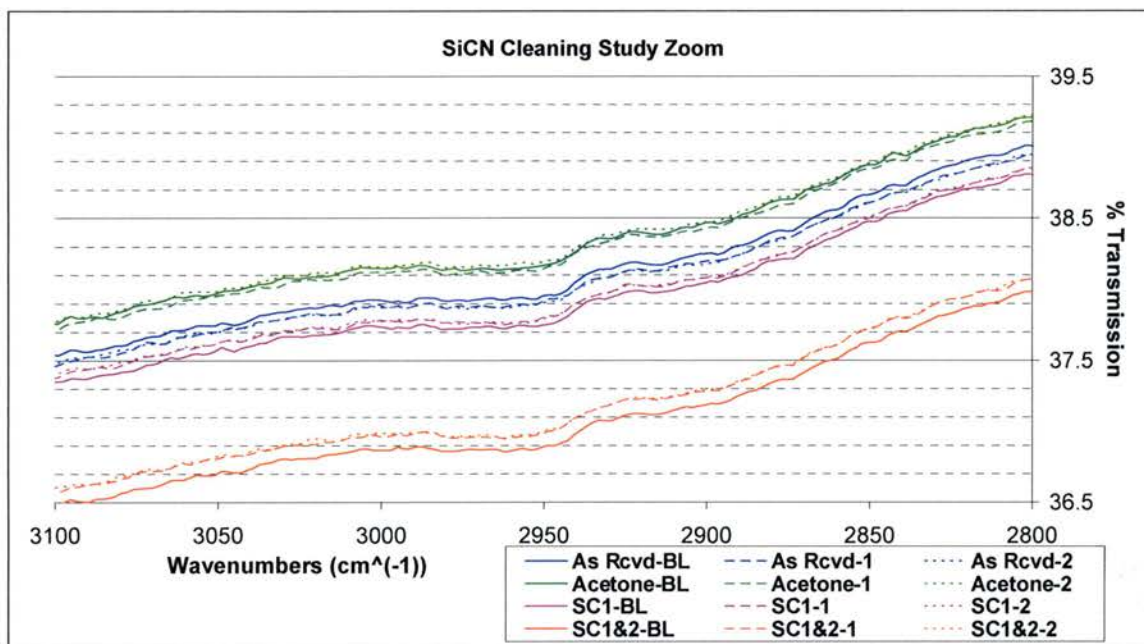


Figure 36 As Rcvd, Acetone, SC1 and SC1&2 all have variation of less than 0.2 this is not indicative of any change to the transmission rate for the substrate due to cleaning. The greatest variation is seen in the transition to different locations in the wafer, this variation approaches 1%.

The AFM analysis of the cleaned samples revealed that the best method of those tried for cleaning SiO₂ substrates is the industry standard SC-1 in combination with SC-2 with respect to the final RMS roughness. Our analysis was not designed to measure global etching of the surfaces cleaned since this is documented elsewhere. Our concern was detection of any selective etching of the surface that increased the final RMS roughness. For our test, all of the cleaning methods were effective for SiO₂ in that they reduced the RMS roughness. For our SiC and SiCN samples the best cleaning technique as indicated by RMS roughness varied by size of the area considered. With the 1 μm² area having a slightly smoother surface after an RCA-1 only clean and the 5 μm² area being moderately smoother after the acetone bath. Realistically though, without a clean room environment to work in and with out a pre-clean RMS roughness for each individual sample none of our samples showed any adverse effect or advantage from any

of the different cleaning methods tested. All of the substrates tested had RMS roughness between, 1 Å and 6 Å at the 1 μm x 1 μm scan size, and 2 Å and 7 Å at the 5 μm x 5 μm scan size.

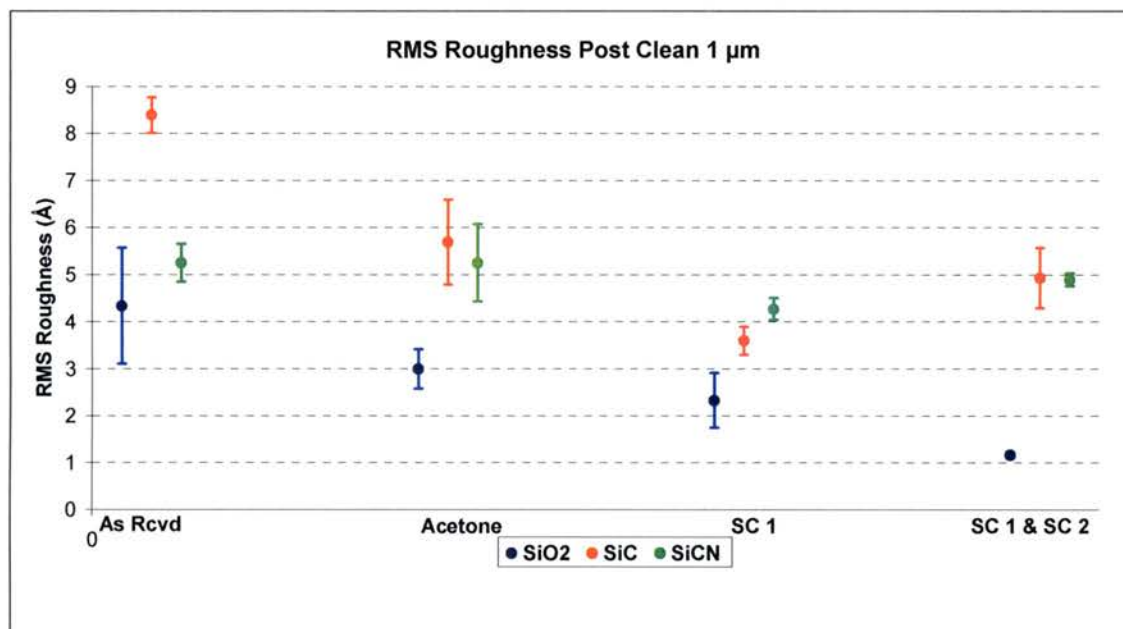


Figure 37 Comparison by AFM of RMS roughness for 1 μm^2 scans after different cleaning methods. Only SiO₂ showed a preferable cleaning method the industry standard of SC-1 and SC-2 in combination.

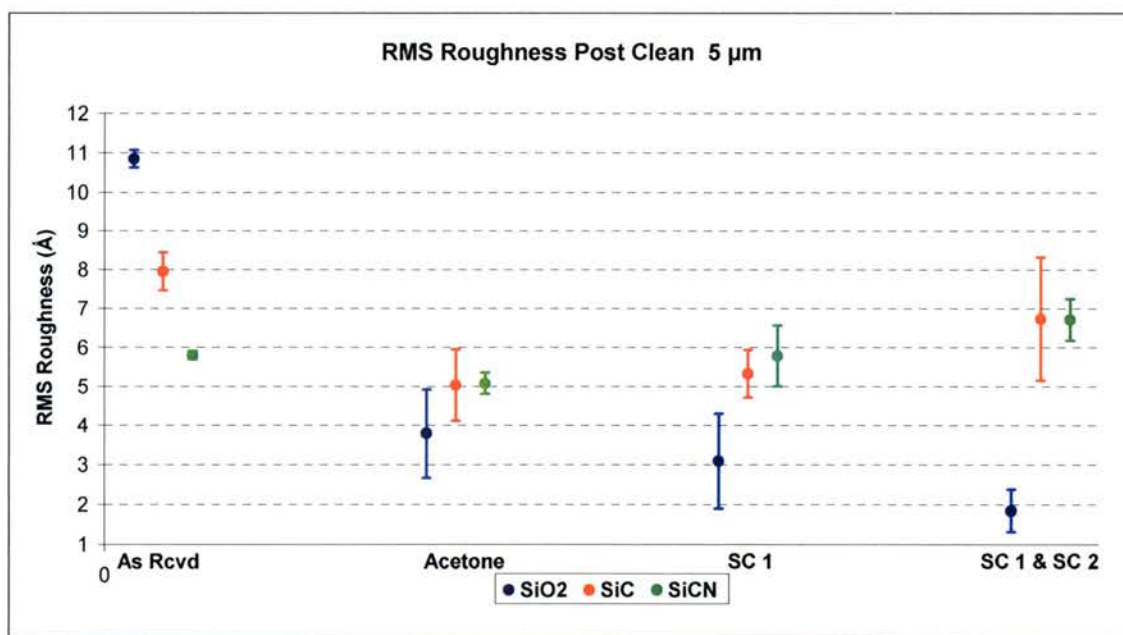


Figure 38 Comparison by AFM of RMS roughness for 5 μm^2 scans after different cleaning methods. Only SiO₂ showed a preferable cleaning method the industry standard of SC-1 and SC-2 in combination.

Random Copolymer Brushes

We were successful in our goal of optimizing the application procedures for our random copolymer (RCP). We optimized the process for P(S-r-MMA) with a molecular number of 8000 - 9000 and 55% PS. The results of our optimization were that a 0.63% by weight solution of RCP in toluene applied via pipette with approximately a 2 mm film and spun at 1000 RPM for 90 seconds is sufficient to provide adequate coverage for a non-preferential surface. We also found that after 8 hours of anneal at 140°C the RCP has a near substrate RMS roughness see figure 39. Also as a part of the qualification of the FTIR, we found that sample orientation has no effect on the intensity of the peaks that represent the RCP. The only variation detected was a global variation in percent transmission that appears to reflect the crystal structure of the substrate.

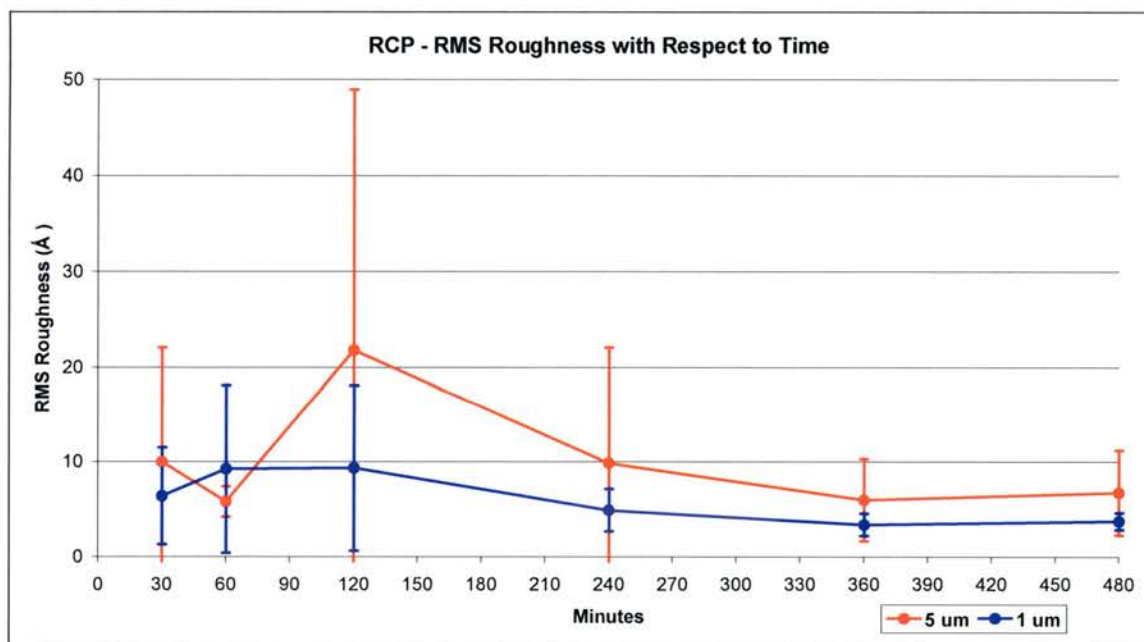


Figure 39 Comparison of RMS roughness for RCP on SiC over 480 minutes of anneal. Our observations showed the RMS roughness of the RCP is stable after 480 minutes and comparable to the RMS roughness of the substrate for both 1 μm x 1 μm and 5 μm x 5 μm scan sizes.

Our second RCP did not have a hydroxyl (OH) tag or termination and did not bond well to any of the substrates. FTIR analysis showed that the RCP without the OH tag failed to remain on the substrate when rinsed with toluene. This was confirmed by AFM analysis, which revealed no change in the nature of the substrate after application of the RCP.

Diblock Copolymer Application

We successfully cast P(S-b-MMA) diblock copolymers of 50.8% PS. Our failure to achieve porous structures from our other two DBCs, with PS ratios of 68.7% appears to confirm the minimum of 70% PS reported in the literature²²⁻²⁴ for formation of PMMA hexagonal arrays. We detected light lamellar structures after annealing the 50.8% PS diblock copolymer for as little as 6 hours. The optimum structures were detected after 18 hours with little or no change after annealing for 48 hours. AFM topographical data revealed average diameters for the lamellar structures of 373 Å. The minimum diameter measured was 239 Å and the maximum was 477 Å. Measurements made in the same region of the sample had standard deviations of approximately 20 Å.

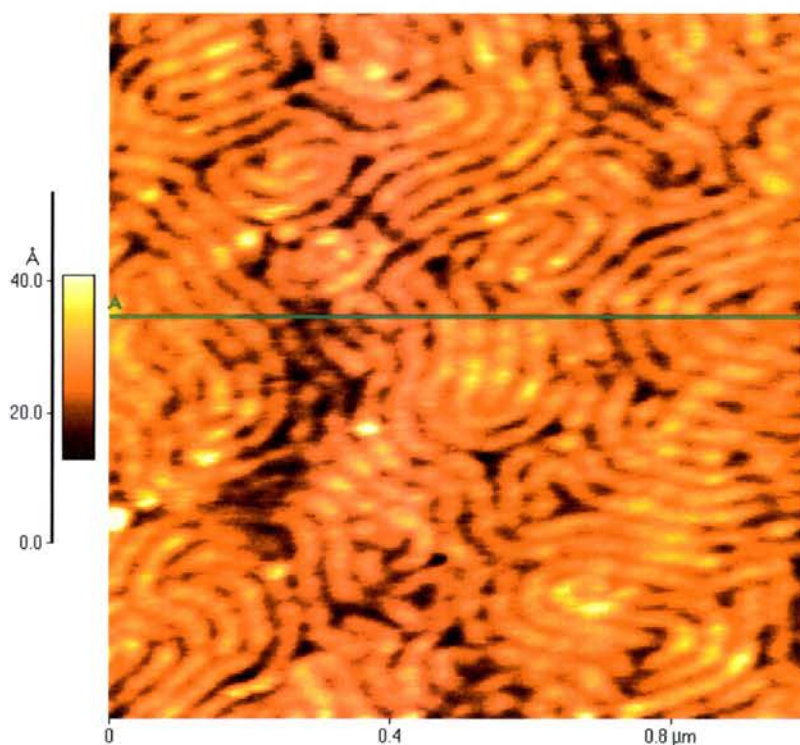


Figure 40 50.8% PS diblock on SiC substrate. The bright lamellar structures are believed to be PMMA.⁴⁶ The color scale to the left shows how the colors represent the height of the structures.

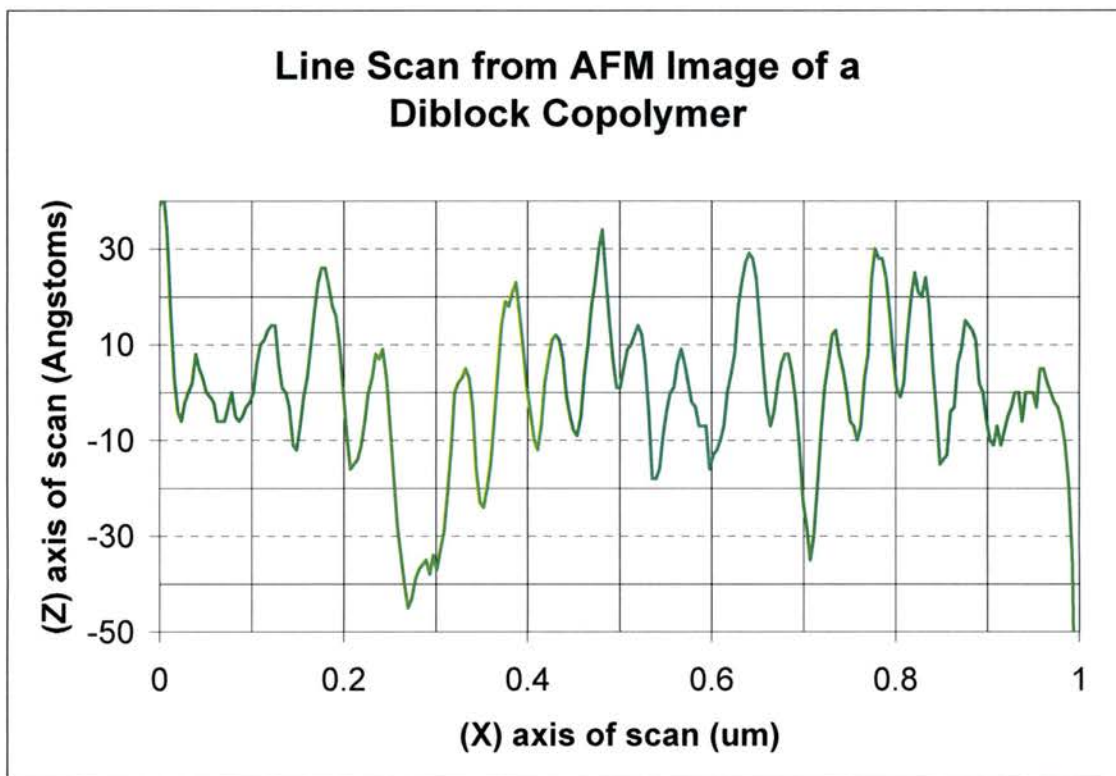


Figure 41 A single line extracted from under the green line in figure 40 at the point of the green line on the scan. The peaks that exceed -30 \AA are presented as dark areas in figure 40.

CHAPTER 5

CONCLUSIONS

We were successful in our investigation into the necessity of and methods for substrate cleaning. We found that ultrasonic cleaning with an acetone bath is an acceptable cleaning method when compared to SC-1 and SC-2 for SiC, SiCN, and SiO₂. Our results showed comparable organic contaminant removal as well as less surface damage, as gauged by AFM RMS roughness measurements, for both SiC and SiCN. An additional benefit of the ultrasonic cleaning is the elimination of the DI H₂O requirement of the Standard Cleans. The ultrasonic cleaning process also requires approximately one-fifth the time to clean an equal number of samples.

Second, we successfully optimized the procedures for application of RCP brushes with a 55% PS concentration and M_n of 8000-9000. Finding a minimum anneal time of 8 hours to return RMS surface roughness comparable to that of a clean substrate. As an element of this process, we showed that FTIR is an acceptable method for verification of deposition of RCP.

We experienced limited success with the application of our 50.8% PS diblock copolymer and showed that there is no detectable self-assembly in a P(S-b-MMA) diblock copolymer where the PS ratio is 68.7%. This agrees with the literature available for P(S-b-MMA) although there is no discussion of our 68.7% concentration. We are

confident that our results confirm the necessity of a 70 % PS concentration for the formation of the hexagonal arrays of PMMA. All future work should include the application of percolation theory to verify the suitability of the diblock copolymer concentration for use in a porous structure. The sporadic success of our 50.8 % PS diblock copolymer is believed to reflect possible contamination of the glove box used during the initial portion of the research.

Additional study is needed to document the conditions that may have prevented consistent structure formation after deposition of the 50.8% PS diblock copolymer. Second, now that a P(S-b-MMA) with a greater than 70% PS concentration is available, further study into the deposition of porous films may be under taken. Third, an annealing time study of the newly received RCP needs to be accomplished. This study may indicate if the percent PS is a factor in the time required for annealing the RCP, since the M_n are similar between the two RCPs. When successful deposition of porous DBCs is accomplished, electrical characterization will be necessary and the test structures for such a characterization will need to be built.

APPENDIX A

Toluene Distillation

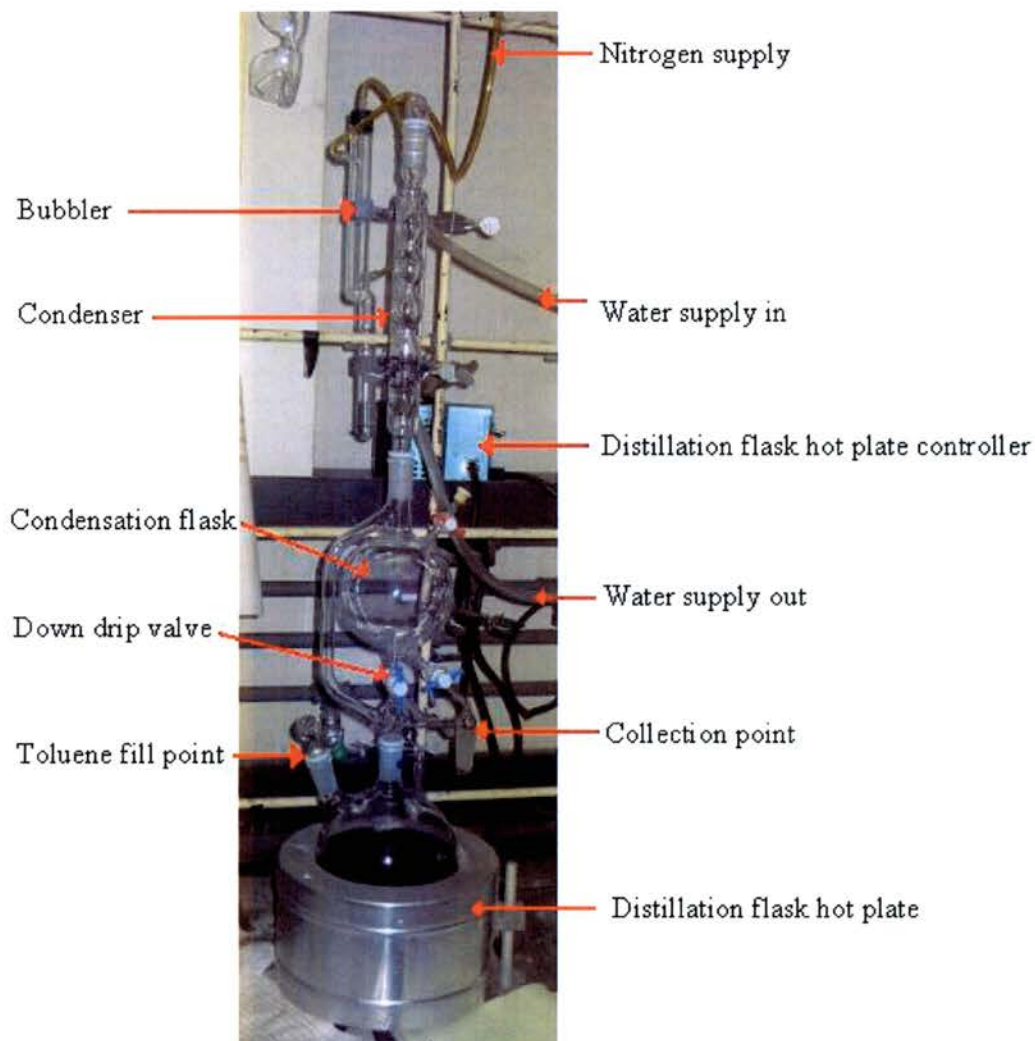


Figure 42 Still used for distillation of chromatographic toluene to produce anhydrous toluene.

These instructions are for a 2-liter distillation flask with a 1-liter condensation flask

1. Still preparation
 - a. Ensure all components are clean
 - b. Na-metal preparation

- i. In a 400 ml beaker place 50-75 ml of Na-metal and enough mineral oil to prevent reaction with H_2O in air
- ii. Add hexane in approximately 50 ml portions stirring with a metal spatula until Na-metal is free of mineral oil
- iii. Siphon off mineral oil using a pipette leaving sufficient hexane to cover Na-metal
- iv. Add isopropanol one pipette at a time until Na-metal is shiny
- v. Ensuring Na-metal is not exposed to moisture pour off hexane and isopropanol and add portions of toluene
- vi. When satisfied that Na-metal is free of hexane and isopropanol transfer toluene and Na-metal to distillation flask.

2. Still operation

- a. Toluene feed stock should be out-gassed before introduction to the still
 - i. Out-gas toluene for approximately 20 minutes using either argon or nitrogen with a slow bubble (argon is the preferred method)
- b. Fill distillation beaker approximately $2/3$ full and return plug
- c. Ensure down drip is open
- d. Purge the still with nitrogen for approximately 10 minutes with approximately 15 psi
- e. Turn off nitrogen purge and heat distillation flask until toluene starts to reflux
- f. Still should be allowed to reflux for at least 24 hrs
- g. Add 1-2 ml of Benzophenone to distillation flask
 - i. If toluene turns blue or purple in color still is ready for use

- ii. If no color change allowed to reflux longer
 - h. To decant toluene from still close the down drip valve
 - i. It may be necessary to increase the heat to the distillation flask
 - i. Allow approximately 75 ml to collect in condensation flask
 - j. Turn on nitrogen at approximately 10 psi and drain of toluene this will be disposed of to insure any contaminants more volatile than the toluene have been removed
 - k. Close drain and turn off nitrogen
 - l. Allow desired quantity of toluene to collect in condensation flask
 - m. Turn on nitrogen at approximately 10 psi and drain of toluene
 - n. Close drain and turn off nitrogen
 - o. Ensure down drip is open
 - p. Reduce heat until toluene stops refluxing
 - i. This may take some time
 - q. Refill distillation flask with fresh toluene in accordance with step 2 a
3. The distilled toluene is collected in a clean dry vessel and stored over 75-100 ml of molecular-sieves to help maintain an anhydrous solvent

APPENDIX B

Standard Clean Procedures

1. Chemicals

Chemicals Used for Standard Cleans (SC-1 & SC-2)	
Deionized H ₂ O	10 MΩ cm resistivity or better
NH ₄ OH	27-30%
H ₂ O ₂	27-30%
HCl	27-30%

Table 8 Chemical requirements for standard cleans

2. SC-1

- a. Solution is 5 parts deionized H₂O, 1 part NH₄OH, 1 part H₂O₂
- b. In the solvents hood
- c. Set up a hot plate with a water bath arrangement see figure 42
- d. Heat H₂O to 75-80°C
- e. Add NH₄OH and H₂O₂ and allow to come to a vigorous bubble
- f. Submerge sample to be cleaned for 10-15 minutes
- g. When sample is removed it should be rinsed in flowing DI water until the resistivity of the runoff matches or is close to the resistivity of the supply
i.e. runoff resistance of 8-9 MΩ ≈ supply resistivity of 13.9 MΩ cm which yields an 8-9 MΩ resistance in a 9 cm petri dish
 - I) Ohm meter probes are clamped to the apposing sides of a 9 cm petri dish
 - II) The runoff is allowed to flow into this Petri dish and resistance of the run off is measured

III) When the runoff is $\approx 9 \text{ M}\Omega$ the rinse is complete (this is the experimental value for the runoff prior to rinsing of sample)

3. SC-2

- a. Solution is 6 parts deionized H_2O , 1 part HCl , 1 part H_2O_2
- b. In the solvents hood
- c. Set up a hot plate with a water bath arrangement see figure 42
- d. Heat H_2O to $75\text{-}80^\circ\text{C}$
- e. Add HCl and H_2O_2 and allow to come to a vigorous bubble
- f. Submerge sample to be cleaned for 15 minutes
- g. When sample is removed it should be rinsed in flowing DI water until the resistivity of the runoff matches or is close to the resistivity of the supply
i.e. runoff resistance of $8\text{-}9 \text{ M}\Omega \approx$ supply resistivity of $13.9 \text{ M}\Omega \text{ cm}$ which yields an $8\text{-}9 \text{ M}\Omega$ resistance in a 9 cm petri dish
 - I) Ohm meter probes are clamped to the apposing sides of a 9 cm petri dish
 - II) The runoff is allowed to flow into this Petri dish and resistance of the run off is measured
 - III) When the runoff is $\approx 9 \text{ M}\Omega$ the rinse is complete (this is the experimental value for the runoff prior to rinsing of sample)

Note: Service life on both solutions is approximately 30 minutes at $75\text{-}80^\circ\text{C}$

Shelf life of room temperature solutions is less than 24 hours

4. Clean up

- a. Allow solutions to cool to room temperature
- b. Dump remaining SC-1 solution into base waste barrel
- c. Dump remaining SC-2 solution into acid waste barrel
- d. Using soap and water clean all glass ware
- e. Triple rinse all glassware with DI and place on drying rack

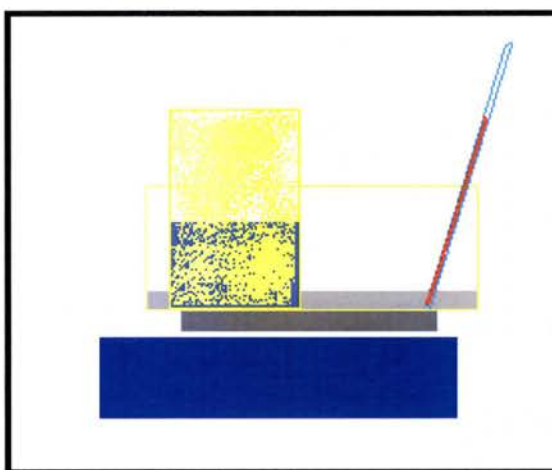


Figure 43 Hot plate with water bath and standard clean solution.

APPENDIX C

Spinner Operation

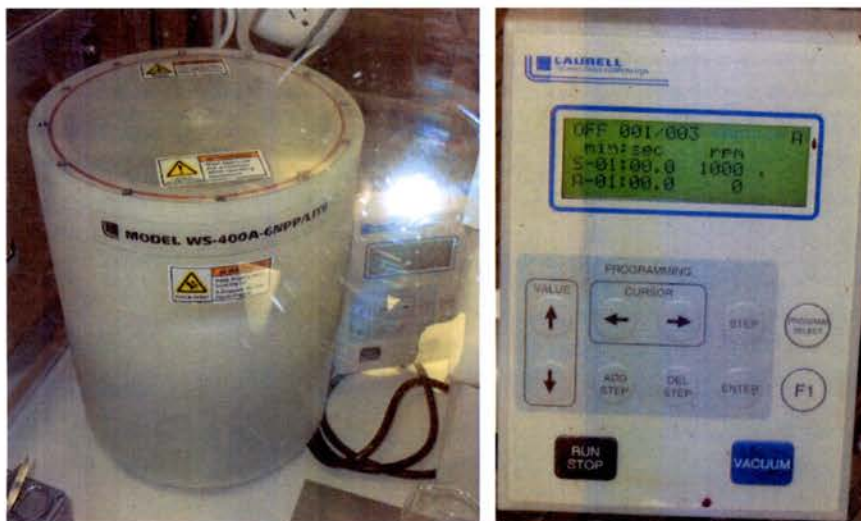


Figure 44 Spinner in glove box and control panel.

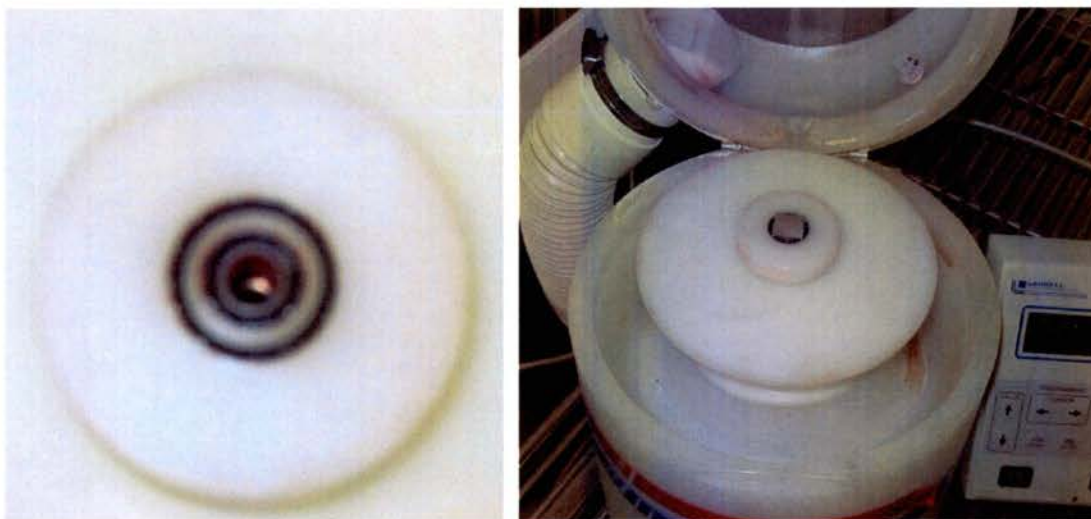


Figure 45 Spinner vacuum chuck without and with sample.

- Power requirements 120 v 60 Hz
- Additional support equipment vacuum pump

1) Spinner Programming

- A) Turn on power and vacuum supply

B) Select the appropriate program or an unused one by pressing the “select program“ button

- i) There are 26 possible programs (A-Z)
- ii) Each program may have up to six steps programmed
- iii) To review or modify program steps press the F1 button

C) Program modification

i) Spin time modification (**S**)

- (1) Using the left/right keys move the cursor to the setting you wish to modify
- (2) Using the up/down keys you may modify the settings

ii) Spin RPM modification (**S**)

- (1) Using the left/right keys move the cursor to the setting you wish to modify
- (2) Using the up/down keys you may modify the settings

iii) Spin acceleration modification (**A**)

- (1) Using the left/right keys move the cursor to the setting you wish to modify
- (2) Using the up/down keys you may modify the settings

iv) Step modification

- (1) Use either the add or remove step buttons and repeat the spin, RPM, and acceleration steps

2) Spinner Operation

A) Raise the lid and place a sample on the vacuum chuck

B) Lower the lid and activate the vacuum the reading should be > than 22 inches of Hg

C) Apply the liquid you wish to spin cast and press the start button

D) When the spinner rpm returns to zero the operation is complete

E) Deactivate the vacuum chuck and raise the lid

F) Remove your sample and repeat as necessary

3) Spinner shut-down

A) Using a lint free towel clean any remaining liquid from the interior of the spinner

B) Turn of the power and the vacuum pump

APPENDIX D

Glove Box Operation



Figure 46 (left) Glove box with all tools inside and controllers on top. (right) Humidity controller *Nitro watch* and gas supply control *Dual Purge*.

- Facility requirements
- Power supply 120 v 60 Hz

Gas:					
Compressed Nitrogen (N ₂)				Purity 99.998%	
O ₂	0.11 ppm	CO ₂	> 0.06 ppm	H ₂	> 0.08 ppm
H ₂ O	> 0.08 ppm	CO	0.15 ppm	THC	> 0.1 ppm

Table 9 Compressed Gas Specifications for use with glove box

- Internal positive pressure is maintained between 1-4 inches of H₂O (0.036-0.144 psi) to prevent moisture and oxygen from entering the chamber
- 1) Control Systems
 - A) The nitro watch is used to maintain a pre-selected % relative humidity (RH)
 - B) N₂ supply should be set at 30 psi on the Dual Purge regulator
 - C) The desired % RH is set on the nitro watch system using the up/down buttons
 - D) If you select a setting below the current RH an alarm will sound, to cancel the alarm just press any button on the control panel

2) Use of the glove box

- A) Materials are introduced to the chamber via the anti chamber
- B) Items to be introduced to the glove box should be placed in the anti chamber
- C) Close the anti chamber and turn on the manual 20 SCFH to purge the anti chamber for approximately 10 minutes
- D) When purge is completed open the interior door
- E) Allow glove box to continue purging for another 10 minutes or until the RH has dropped below the desired operating level whichever takes longer
- F) To protect the glove box from damage all operations should be performed over the aluminum work surface

APPENDIX E

Ultrasonic Cleaner Operation

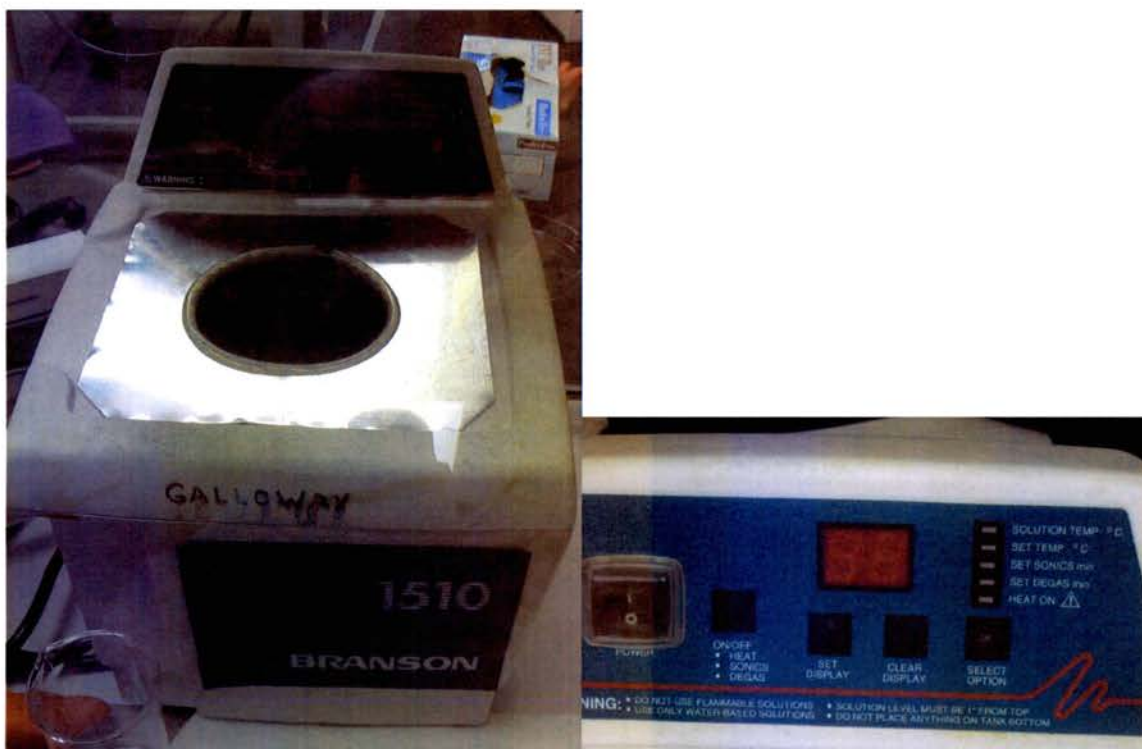


Figure 47 Ultrasonic Cleaner, the reservoir is filled with silicone oil to prevent evaporation and contamination of the nitrogen environment (left) View of control panel for tool (right).

- Power supply 120 v 60 Hz
- For operation in the low oxygen environment the reservoir is filled with silicon oil rather than DI H₂O

1) Operation

- A) Turn on power and select the mode of operation (set sonics)
- B) Set the timer to the desired operating period (5 min)

- **Care must be exercised to prevent damage to the glove box from solvent spills, always work over the aluminum work surface**

- C) Place a 500 ml beaker in the opening and add approximately 150 ml of acetone
- D) Put substrate sample in the acetone
- E) Start sonic cycle you can hear a rattle in a quiet room if not look for ripples in the acetone to indicate operation of the ultrasonic cleaner

- **Care must be exercised to prevent damage to the glove box from solvent spills, always work over the aluminum work surface**
- **Caution silicone oil is easily spread and time consuming to remove from the glove box**

2) Shut down procedures

- A) After cleaning cycle is complete remove the substrates from the acetone as quickly as possible
- B) Once all samples are cleaned, remove the 500 ml beaker from the ultrasonic cleaner and remove from the glove box (a large petri dish lined with a dry towel makes a good drip tray)
- C) Turn off power and replace cover

APPENDIX F

Vacuum Oven Operation



Figure 48 Vacuum or annealing oven. To the left is the vacuum pump, the oven control panel contains power switch, temperature setting, vacuum gauge, and vent/vacuum valves.

- Power requirements 120 v 60 Hz
- Additional support equipment vacuum pump
- Operational range: ambient + 5 °C to 325 °C
- The configuration pictured above may be evacuated to approximately 27 in Hg

1) Oven operation

- A) Before operation insure oven is empty
- B) Set desired temperature using up down buttons on control panel
- C) After desired temperature is reached place sample in oven

- D) Close the vent/purge valve (small knob upper left of control panel)
- E) With vacuum pump running open vacuum valve (large knob upper right of control panel)

2) Oven shut-down or sample retrieval procedures

- A) Close the vacuum valve
- B) Open the purge/vent valve and allow internal pressure to reach atmospheric pressure
- C) Open door remove samples (**Samples may be HOT**)
- D) To shut down turn off oven
- E) Turn off vacuum pump, leaving vacuum valve closed

APPENDIX G

Polymer Preparation

- **Protect all polymers from moisture (especially RCP)**
 - **Protect all polymers from light**
1. Sample bottles should be thoroughly washed with soap and water rinsed with acetone and allowed to air dry
 2. Rinse again with toluene and allow to air dry
 3. Place dry bottles in vacuum oven at 110 °C for 2 hrs
 4. Cap bottles immediately on removal from vacuum oven
 5. Put sample bottles in the glove box reduce humidity to < 10% Relative Humidity (RH) and store uncapped bottles in nitrogen for a minimum of 4 hrs (this is to remove any moisture introduced during removal from oven)
 6. Cap the sample bottles and remove for empty bottle weighing
 7. Return empty bottles to the glove box and allow humidity to return to < 10 % RH
- **You should turn off the gas flow to reduce the possibility of spilling the polymers**
8. Add a small amount of polymer (0.02-0.07 grams) to the sample jars and recap the jars
 9. Reset gas supply for < 10 % RH and remove the sample bottles for weighing
 10. After weighing return bottles to glove box and let RH return to, 10%
 11. Add anhydrous toluene (see still procedures Appendix A) to sample bottles for 1% by weight solutions, Except RCP. RCP is a 0.63% by weight solution
 - a. $[(\text{Mass of polymer}) \times (100)] / (\text{solution percentage}) = \text{toluene in ml to be added}$

12. Clean samples using the ultrasonic cleaner in the glove box with acetone bath
13. Approximately 0.5 ml of the solution is applied via pipette to the substrate on the spinner
14. After spin drying the sample is annealed and rinsed with toluene
15. The sample is then returned to the glove box and the humidity is reduced to < 10% RH
16. Approximately 0.5 ml of the solution is applied via pipette to the substrate on the spinner
17. After spin drying the sample is annealed and rinsed with toluene
18. The samples are exposed to UV to degrade the PMMA and promote cross-linking of the PS
19. The sample is then soaked in galactic acetic acid a selective solvent for PMMA

REFERENCES

- a Permanent Address: willowowisp@gmail.com
 - b K. Miller; “Additive Methods in Molecular Polarizability”; Journal of the American Chemical Society; 112, (1990)
 - c AIP Physics Desk Reference, 3rd ed.; edited by E. Cohen, D. Lide, G. Trigg; (Springer, N.Y.; 1983); p 380, 685
 - d P. Ho, J. Leu, W. Lee; Low Dielectric Constant Materials for IC Applications; (Springer-Verlag, Berlin Heidelberg, 2003); p 6
 - e E. Penzel, J. Rieger, H. Schneider; “The Glass Transition Temperature of Random Copolymers: 1. Experimental Data and the Gordon-Taylor Equation”; Polymer, 38, No. 2, (1996)
1. S. Chan, K. Shepard; “Practical Considerations in RLCK Crosstalk Analysis for Digital Integrated Circuits”, Proceedings of the (2001) International Conference on Computer Aided Design
 2. Q. Xu, P. Mazumder, Z. Li; “Transmission Line Modeling by Modified Method of Characteristics”; Proceedings of the 14th International Conference on VLSI Design
 3. K. Agarwal, D. Sylvester, D. Blaauw; “A Simplified Transmission-Line Based Crosstalk Noise Model for On-Chip RLC Wiring”; Proceeding of the (2004) Asia and South Pacific Design Automation Conference
 4. L. Pileggi; “Coping with RC(L) Interconnect Design Headaches”; Proceedings of the (1995) International Conference on Computer Aided Design
 5. G. Zhong, C. Koh, K. Roy; “On-Chip Interconnect Modeling by Wire Duplication”; Proceedings of the (2002) International Conference on Computer Aided Design
 6. Y. Lu, M. Celik, T. Young, L. Pileggi; “Min/Max On-Chip Inductance Models and Delay Metrics”; Proceeding of the 38th Design Automation Conference
 7. F. Dartu, L. Pileggi; “Calculating Worst-Case Gate Delays Due to Dominant Capacitive Coupling”; Intel corp. and Semiconductor Research corp.; (1997)

8. M. Kamon, S. McCormick, K. Shepard; "Interconnect Parasitic Extraction in the Digital IC Design Methodology"; Proceedings of the (1999) International Conference on Computer Aided Design
9. P. Ho, J. Leu, W. Lee; Low Dielectric Constant Materials for IC Applications; (Springer-Verlag, Berlin Heidelberg, 2003); pp 1-19
10. D. Stroud; "The Effective Medium Approximations: Some Recent Developments"; Supperlattices and Microstructures, 23; No 24 (1998)
11. R. Howard, L. Benatar; A Practical Guide to Scanning Probe Microscopy; Copyright (1993-2000 Thermo Microscopes); p 9
12. SPM Training Notebook; (Copyright 2003 Veeco Instruments Inc); pp 8-13
13. D. Skoog, D. West; Principles of Instrumental Analysis; (Holt, Rienhart and Winston Inc. Copyright 1971); pp 131-168
14. J. Coates; Interpretation of Infrared Spectra, A Practical Approach; (John Wiley & Sons LTD, Chichester, 2000); pp 2-10
15. T. Thurn-Albrecht, J. Schotter, G. Kastle, et al.; "Ultrahigh-Density Nanowire Arrays Grown in Self-Assembled Diblock Copolymer Templates"; Science, 290, (2000)
16. T. Thurn-Albrecht, R Steiner, J. DeRouchey, et al.; "Nanosopic Templates from Oriented Block Copolymer Films"; Adv Materials,, 12, no. 11, (2000)
17. C. Park, J. Kim, M. Ree, et al.; "Thickness and Composition Dependence of the Glass Transition Temperature in Thin Random Copolymer Films"; Polymer 45, (2004)
18. G. Strobl; The Physics of Polymers; 2 nd ed.(Springer-Verlag, Berlin, Germany, 1997); pp 231-243
19. E. Penzel, J. Rieger, H. Schneider; "The Glass Transition Temperature of Random Copolymers: 1. Experimental Data and the Gordon-Taylor Equation"; Polymer, 38, No. 2, (1996)
20. C. Gigault, K. Dalnoki-Veress, J. Dutcher; "Changes in the Morphology of Self-Assembling Polystyrene Microsphere Monolayers Produced by Annealing"; Journal of Colloid and Interface Science, 243, (2001)
21. S. Milner; "Polymer Brushes"; Science, 251, (1999)
22. P. Mansky, Y. Liu, E. Haung, T. Russel, C. Hawker; "Controlling Polymer-Surface Interactions with Random Copolymer Brushes"; Science, 275, (1997)

23. Mansky, T. Russel, C. Hawker, et al.; "Ordered Diblock Copolymer Films on Random Copolymer Brushes"; *Macromolecules*, 30, (1997)
24. E. Huang, L. Rockford, T. Russel, C. Hawke; "Nanodomain Control in Copolymer Thin Films"; *Nature*, 395, (1998)
25. B. Zhao, R. Haasch, S. MacLaren; "Self-Reorganization of Mixed Poly(Methyl Methacrylate)/Polystyrene Brushes on Planar Silica Substrates in Response to Combined Selective Solvent Treatments and Thermal Annealing"; *Polymer*; 45; (2004)
26. W. Whitaker; "Self-Assembling Diblock Copolymers as Mask for Reactive Ion Etching"; National Nanofabrication Users Network
27. M. Misner, H. Skaff, T. Emrick, T. Russel; "Directed Deposition of Nanoparticles Using Diblock Copolymer Templates"; *Adv. Materials*, 15, no 3, (2003)
28. E. Haung, S. Pruzinsky, T. Russel, et al.; "Neutrality Conditions for Block Copolymer Systems on Random Copolymer Brush Surfaces"; *Macromolecules*, 23, (1999)
29. C. Black, K. Guarni, K. Milkove, et al.; "Integration of Self-Assembled Diblock Copolymers for Semiconductor Capacitor Fabrication"; *Applied Physics Letters*, 79, No 3, (2001)
30. U. Jeong, D. Ryu, J. Kim, et al.; "Volume Contractions Induced by Crosslinking: A Novel Route to Nanoporous Polymer Films"; *ADV Materials*, 15, No. 15, (2003)
31. T. Xu, H. Kim, J. DeRouchey, et al.; "The Influence of Molecular Weight on Nanoporous Polymer Films"; *Polymer*, 42, (2001)
32. C. Black, K. Guarini; "Self Assembly Kinetics of Cylindrical-Phase Diblock Copolymer Thin Films"; IBM Research Report RC22700 (W0301-087) (unpublished)
33. H. Wang, A. Djurisc, M. Xie, et al.; "Perpendicular Domains in Poly(Styrene-b-Methyl Methacrylate) Block Copolymer Films on Preferential Surfaces"; *Thin Solid Films*, 488, (2005)
34. Handbook of Semiconductor Wafer Cleaning Technology, edited by Werner Kern, (Noyes Publications, Park Ridge, New Jersey 1993); pp 14-56
35. I. Kashkoush, R. Novak; E. Brause; "In-Situ Chemical Concentration Control for Wafer Wet Cleaning," *Journal of the IEST* 41 no3, (1998)
36. M. Knotter; "Challenges for Surface Preparation 2004"; Philips Semiconductors Nijmegen; presented at the Wafer Clean & Surface prep Conference; Austin, Texas; May 2004; (unpublished)

37. C. Cetikaya; presented at the Wafer Clean & Surface prep Conference; Austin, Texas; May 2004; (unpublished)
38. K. Derbyshire; "Study Finds RCA Clean Still the Best Solution," *Solid State Technology*; 38, 6, (1995)
39. Handbook of Semiconductor Wafer Cleaning Technology, edited by Werner Kern, (Noyes Publications, Park Ridge, New Jersey 1993); pp 25, 412-414
40. P. Mertens, K. Marent; "Single Wafer Wet Cleaning Improved by Novel High Performance Wafer Drying," *Solid State Technology*; September (2000)
41. A. Busnaina, F. Dai; "Megasonic Cleaning"; *Semiconductor International*; (1997)
42. L. Rockford, Y. Liu, P. Mansky, T. Russel; "Polymers on Nanoperiodic, Heterogeneous Surfaces"; *Physical Review Letters*, 82 No. 12, (1999)
43. Nicolet FT-IR User's Guide; (Copyright 2004 Thermo Electron Corporation) pp 67-70
44. B. Ro, T. Dawson; "The role of Sebaceous Gland Activity and Scalp Microfloral Metabolism in the Etiology of Seborrheic Dermatitis and Dandruff"; *The Journal of Investigative Dermatology Symposium Proceedings*, 10, 3, (2005)
45. Handbook of Semiconductor Wafer Cleaning Technology, edited by Werner Kern, (Noyes Publications, Park Ridge, New Jersey 1993); pp 18 - 39, 357, 517 - 519
46. T. Morkved, W. Lopes, J. Hahm, et al.; "Silicon Nitride Membrane Substrates for the Investigation of Local Structure in Polymer Thin Films"; *Polymer*, 39, No. 16, (1998)

IMAGE REFERENCES

- Figure 2,3,5 A Practical Guide to Scanning Probe Microscopy; (Copyright 1993-2000 ThermoMicroscopes); pp 12, 35, 37
- Figure 6 A Practical Guide to Scanning Probe Microscopy; (Copyright 1993-2000 ThermoMicroscopes); p 19
- Figure 9-11 MDL models; NIST Chemistry Webbook;
<<http://webbook.nist.gov/chemistry/>>
- Figure 12 Adapted from M. Knotter; “Challenges for Surface Preparation 2004”; Philips Semiconductors Nijmegen; presented at the Wafer Clean & Surface prep Conference; Austin, Texas; May 2004; (unpublished)
- Figure 13, 14 Handbook of Semiconductor Wafer Cleaning Technology, edited by Werner Kern, (Noyes Publications, Park Ridge, New Jersey 1993) pp 413, 414
- Figure 15 (left) M. Plesset, R. Chapman; “Collapse of an initially spherical vapor cavity in the neighborhood of a solid boundary”; *Journal of Fluid Mechanics*, 47, (1971)
(right) L. Crum; “Surface Oscillations and Jet Development in Pulsating Bubbles”; *Canadian Journal of Physics*; 40 (1979)

VITA

William Thomas Gibson was born in Temple, Texas on June 25, 1966, the son of Doris Osborn Gibson and Jack Thomas Gibson. William graduated from Temple High School in 1984 to become a part time student. He served in the U.S. Air Force for seven years separating in 1995. In 1999 he returned to school, receiving an Associates of Science from Blinn College in 2000, and a Bachelors of Science from Texas State University-San Marcos in 2003. And, entered the Graduate College of Texas State University-San Marcos in June 2003.

Permanent Address: 1640 Aquarena Springs Drive Apt 302
San Marcos, Texas 78666

This thesis was typed by William Thomas Gibson